UNIVERSITÄT AUGSBURG
Universitätsbibliothek

OPEN ACCESS
OPUS AUGSBURG

Two-resonator circuit quantum electrodynamics: dissipative theory

Georg M. Reuther, David Zueco, Frank Deppe, Elisabeth Hoffmann, Edwin P. Menzel, Thomas Weißl, Matteo Mariantoni, Sigmund Kohler, Achim Marx, Enrique Solano, Rudolf Gross, Peter Hänggi

Angaben zur Veröffentlichung / Publication details:

Reuther, Georg M., David Zueco, Frank Deppe, Elisabeth Hoffmann, Edwin P. Menzel, Thomas Weißl, Matteo Mariantoni, et al. 2010. "Two-resonator circuit quantum electrodynamics: dissipative theory." *Physical Review B* 81(14): 144510. https://doi.org/10.1103/physrevb.81.144510.

Nutzungsbedingungen / Terms of use:

licgercopyright

Dieses Dokument wird unter folgenden Bedingungen zur Verfügung gestellt: / This document is made available under these conditions:
Deutsches Urheberrecht
Weitere Informationen finden Sie unter: / For more information see:
https://www.uni-augsburg.de/de/organisation/bibliothek/publizieren-zitieren-archivieren/publiz/

Two-resonator circuit quantum electrodynamics: Dissipative theory

Georg M. Reuther,[1,*] David Zueco,[1,†] Frank Deppe,[2] Elisabeth Hoffmann,[2] Edwin P. Menzel,[2] Thomas Weißl,[3] Matteo Mariantoni,[2,3,‡] Sigmund Kohler,[4] Achim Marx,[2] Enrique Solano,[5,6] Rudolf Gross,[2] and Peter Hänggi[1]

[1]*Institut für Physik, Universität Augsburg, Universitätsstraße 1, D-86135 Augsburg, Germany*

[2]*Walther-Meißner-Institut, Bayerische Akademie der Wissenschaften, Walther-Meißner-Str. 8, D-85748 Garching, Germany*

[3]*Physik-Department, Technische Universität München, James-Franck-Str., 85748 Garching, Germany*

[4]*Instituto de Ciencia de Materiales de Madrid, CSIC, Cantoblanco, E-29049 Madrid, Spain*

[5]*Departamento de Química Física, Universidad del País Vasco-Euskal Herriko Unibertsitatea, Apdo. 644, 48080 Bilbao, Spain*

[6]*IKERBASQUE, Basque Foundation for Science, Alameda Urquijo 36, 48011 Bilbao, Spain*

(Received 13 November 2009; revised manuscript received 30 January 2010; published 20 April 2010)

We present a theoretical treatment for the dissipative two-resonator circuit quantum electrodynamics setup referred to as quantum switch. There, switchable coupling between two superconducting resonators is mediated by a superconducting qubit operating in the dispersive regime, where the qubit transition frequency is far detuned from those of the resonators. We derive an effective Hamiltonian for the quantum switch beyond the rotating-wave approximation and provide a detailed study of the dissipative dynamics. As a central finding, we derive analytically how the qubit affects the quantum switch even if the qubit has no dynamics, and we estimate the strength of this influence. The analytical results are corroborated by numerical calculations, where coherent oscillations between the resonators, the decay of coherent and Fock states, and the decay of resonator-resonator entanglement are studied. Finally, we suggest an experimental protocol for extracting the damping constants of qubit and resonators by measuring the quadratures of the resonator fields.

DOI: 10.1103/PhysRevB.81.144510 PACS number(s): 84.30.Bv, 03.67.Lx, 32.60.+i, 42.50.Pq

I. INTRODUCTION

Circuit quantum electrodynamics[1–3] (QED) is the solid-state analog of quantum-optical cavity QED.[4–6] While in the latter natural atoms are coupled to three-dimensional cavities, the former is based on superconducting quantum circuits and the roles of the atoms and the cavities are played by qubit[7–9] and microwave resonator circuits,[10–12] respectively. In fundamental research, circuit QED architectures have proved to be valuable for implementing quantum optics on a chip, for which a rich toolbox has been developed.[13–22] These experiments were based on a single qubit coupled to a single resonator. With applications for quantum information processing in mind, an extension to multiple qubits seems natural.[23–26] More recently, the potential of using multiple resonators has been pointed out by several authors.[27–29]

Under opportune circumstances, in a two-resonator circuit QED setup, a superconducting qubit acts as a quantum switch between two superconducting on-chip resonators.[27] To this end, the qubit must be detuned from both resonators. The resulting effective Hamiltonian describes a resonator-resonator interaction whose coefficient has two contributions. The first contribution depends on the qubit state and the qubit-resonator detuning and can have a positive or negative sign. The second one has a definite sign and stems from the fact that qubit and resonators are not pointlike objects but extended circuits. Provided that the qubit always is in a suitable energy eigenstate, the switch is turned off when both terms are balanced and turned on otherwise. Beyond this simple protocol, the "quantumness" of the setup can be exploited by bringing the qubit into a superposition state with the resonators. This allows for generating bipartite and tripartite entanglement or Schrödinger cat states.

In a real experiment, one expects the operation of the two-resonator circuit QED setup to be affected by the various decoherence rates of qubit and resonators. Since most implementations of superconducting qubits can be tuned by external parameters, those rates depend not only on the qubit type, but also on the operating point. So far,[30–34] they have been in the range of approximately 1–200 MHz. In the case of the quantum switch, only qualitative estimates on the effect of qubit dephasing exist.[27] However, a detailed quantitative understanding of the possible effects stemming from the various existing decoherence channels is indispensable for successful experimental implementation. In particular, it is essential to analyze the effect of qubit decoherence sources on the coupled resonator pair. Hence, in this work, we develop a complete dissipative theory for a circuit QED setup consisting of two resonators both dispersively coupled to a single qubit. As a central result, we demonstrate that qubit relaxation affects the resonators in second dispersive order, whereas dephasing becomes an issue only in fourth dispersive order.

The paper is structured as follows. In Sec. II, we introduce the system Hamiltonian and add the baths causing dissipation to the system. We model the bath influence using a Bloch-Redfield quantum master equation. Next, in Sec. III B, we derive an effective system Hamiltonian beyond the rotating-wave approximation (RWA). We show that this extension results in quantitative, but not qualitative changes compared to a treatment within RWA. Furthermore, in Sec. III C, we derive a simplified effective quantum master equation suitable for analytical treatments. In particular, we use the latter result to compute an explicit expression for the influence of the qubit dissipation channel on the two-resonator system. Sec. IV contains numerical results for various prototypical operation modes of the quantum switch setup. These include coherent oscillations between the resonators, the decay of Fock and coherent states, and the decay of resonator-resonator entanglement. We show that the agree-

 ©2010 The American Physical Society

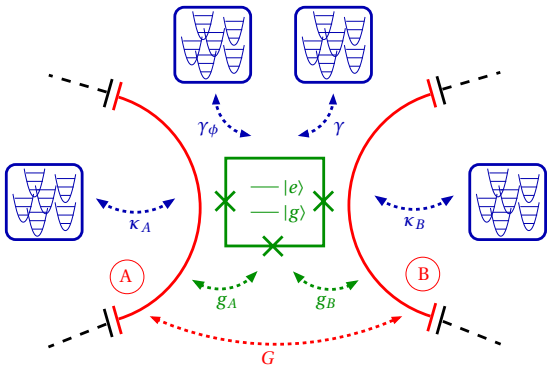

FIG. 1. (Color online) Sketch of the two-resonator circuit QED system under analysis, including schematically the interaction with bosonic heat baths (blue boxes with oscillator potentials). Either microstrip or coplanar waveguides could be employed as resonators (red lines). As in the text, the coupling qubit is exemplarily depicted as persistent-current flux qubit (green loop). The system is coupled to external circuits via coupling capacitors. The decay rates $\kappa_{\{A,B\}}$, γ and γ_ϕ are defined in Sec. II C.

ment with the analytical results obtained by means of the effective quantum master equation of Sec. III C is excellent. Most importantly, we show that qubit dissipation affects the switch only in second dispersive order. Finally, in Sec. V, we suggest a protocol to extract the damping constants of the system by measuring the field modes of the resonators. The appendices contain technical details about the calculations presented in this article.

II. DISSIPATIVE TWO-RESONATOR CIRCUIT QED

We introduce a dissipative description for a circuit QED architecture consisting of two on-chip microwave resonators that are simultaneously coupled to one superconducting qubit. This setup is sketched in Fig. 1. We emphasize that our formalism is general in the sense that qubit and resonators can be based on any suitable quantum circuits. However, whenever we need to give numbers, we assume a persistent-current flux qubit[35,36] coupled to two transmission line resonators henceforth.

A. System-bath model

First, we write down the two-resonator circuit QED Hamiltonian. A detailed derivation is given in Ref. 27. The natural reference frame is the laboratory basis, the physical basis of circuits and fields,

$$\mathcal{H}' = \frac{\hbar\varepsilon}{2}\sigma_z' + \frac{\hbar\delta_Q}{2}\sigma_x' + \hbar\Omega_A a^\dagger a + \hbar\Omega_B b^\dagger b + \hbar G(a+a^\dagger)(b+b^\dagger) + \hbar g_A\sigma_z'(a+a^\dagger) + \hbar g_B\sigma_z'(b+b^\dagger). \tag{1}$$

The first two terms in the first line of the above Hamiltonian represent the qubit in terms of the standard Pauli operators σ_x' and σ_z'. The controllable energy bias is $\hbar\varepsilon$, and $\hbar\delta_Q$ denotes the minimum level splitting. In the particular case of a flux qubit,[35,36] $\hbar\delta_Q$ is the tunnel splitting, and the energy bias $\hbar\varepsilon = 2i_Q(\Phi_x^{\mathrm{DC}} - \Phi_0/2)$ can be tuned by an externally applied flux Φ_x^{DC}. The quantities i_Q and $\Phi_0 = h/2e$ denote the qubit persistent current and the magnetic flux quantum, respectively. When $\Phi_x^{\mathrm{DC}} = \Phi_0/2$ or, equivalently, $\varepsilon = 0$, the qubit is said to be biased at its degeneracy or optimal point, where it is protected from low-frequency noise to first order. The last two terms in the first line of Eq. (1) represent the two resonators with frequencies Ω_A and Ω_B. Here, a, b and $a^\dagger$, $b^\dagger$ are the annihilation and creation operators of the modes in resonators A and B, respectively. The second line of Eq. (1) describes the geometric coupling between the resonators, which is due to the fact that we are dealing with circuits. The coupling coefficient G contains contributions both from a direct coupling and an interaction that is mediated by the qubit circuit. Finally, the third line of Eq. (1) describes the qubit-resonator coupling terms with coefficients g_A and g_B. As explained in Sec. III B, they give rise to a "dynamical" resonator-resonator coupling under appropriate conditions.

In a real experimental scenario, the two-resonator circuit is unavoidably coupled to an external circuit that is characterized by an impedance $Z(\omega)$. In a quantum mechanical description, this impedance can be modeled by coupling the circuit bilinearly to the modes of an electromagnetic environment consisting of an infinite set of harmonic oscillators.[37,38] Following this route, we obtain a Caldeira-Leggett-type system-bath Hamiltonian,[39–41]

$$\mathcal{H}_{\mathrm{tot}}' = \mathcal{H}' + \sum_\mu Q_\mu \sum_j c_j^\mu (d_{j,\mu}^\dagger + d_{j,\mu}) + \sum_\mu \sum_j \hbar\omega_j^\mu \left(d_{j,\mu}^\dagger d_{j,\mu} + \frac{1}{2} \right). \tag{2}$$

The indices $\mu \in \{A, B, x, z\}$ label the system-bath coupling operators with respect to the different reservoirs the system is coupled to. In detail,

$$Q_A = (a + a^\dagger), \quad Q_x = \sigma_x',$$
$$Q_B = (b + b^\dagger), \quad Q_z = \sigma_z'. \tag{3}$$

The coupling coefficients c_j^μ represent the interaction between the system and the different bath modes with frequencies ω_j^μ, which are described by the bosonic annihilation and creation operators $d_{j,\mu}, d_{j,\mu}^\dagger$. Within the scope of this paper, we consider the noise sources to be uncorrelated. This is justified since the different types of noise are caused by fluctuations of distinct nature. In other words, we assume that the baths are independent, $[d_{i,\mu}, d_{j,\nu}^\dagger] = \delta_{ij}\delta_{\mu\nu}$. We find it noteworthy to mention that for $\mu \in \{x, z\}$ the coefficients c_j^μ depend on the specific implementation of the qubit. For a flux qubit, the dominant noise source is believed to be flux noise,[31–33] which couples to the circuit via the z axis in the laboratory frame.

In order to get more physical insight, we rotate $\mathcal{H}'$ into the qubit energy eigenbasis[42] $\{|g\rangle, |e\rangle\}$, where $|g\rangle$ and $|e\rangle$ denote the flux-dependent qubit ground and excited state, respectively. Using the redefined Pauli operators

$$\sigma_x = |g\rangle\langle e| + |e\rangle\langle g| = \cos\theta\sigma_x' - \sin\theta\sigma_z',$$

$$\sigma_z = |e\rangle\langle e| - |g\rangle\langle g| = \sin\,\theta\sigma_x' + \cos\,\theta\sigma_z', \tag{4}$$

we obtain

$$\mathcal{H} = \frac{\hbar\omega_{\rm qb}}{2}\sigma_z + \hbar\Omega_A a^\dagger a + \hbar\Omega_B b^\dagger b + \hbar G(a+a^\dagger)(b+b^\dagger) + \hbar g_A(\cos\,\theta\sigma_z - \sin\,\theta\sigma_x)(a+a^\dagger) + \hbar g_B(\cos\,\theta\sigma_z - \sin\,\theta\sigma_x)(b+b^\dagger). \tag{5}$$

The flux dependence is now encoded in the qubit energy level splitting $\hbar\omega_{\rm qb}=\hbar(\delta_Q^2+\varepsilon^2)^{1/2}$ and the mixing angle $\theta=\arctan(\delta_Q/\varepsilon)$. The qubit-bath coupling operators are rewritten as

$$Q_x = \sigma_x' = \cos\,\theta\sigma_x + \sin\,\theta\sigma_z,$$

$$Q_z = \sigma_z' = \cos\,\theta\sigma_z - \sin\,\theta\sigma_x. \tag{6}$$

They are defined along the rotated axes determined by the tunneling matrix element $\hbar\delta_Q$ in σ_x' direction, and the energy bias $\hbar\varepsilon$ in σ_z' direction. The system-bath interaction is fully characterized by the spectral densities

$$J_\mu(\omega) = \sum_j |c_j^\mu|^2\delta(\omega_j-\omega). \tag{7}$$

In the case where decoherence is mainly caused by external circuitry, the spectral densities are proportional to the real part of the impedances $\mathrm{Re}[Z_\mu(\omega)]$. In general, internal loss mechanisms are also relevant in superconducting resonators at low powers and low temperatures. They often originate from fluctuators on the resonator surface, which are usually modeled as two-level systems. Thus, we interpret the $J_\mu(\omega)$ in an effective sense in that they include both the effects of external circuitry and internal losses. Our effective description does not cover the so-called excess phase noise though, i.e., low-frequency fluctuations in the resonator frequency itself, which originate from the surface fluctuators as well. As it was pointed out and investigated experimentally,[43,44] this leads to resonator dephasing. While such effects are not included in our modeling of decoherence, we cannot ensure that they will only be of minor importance with respect to operating the two-resonator setup (see below in Sec. III A). In most experimental situations, however, decoherence is predominantly governed by external resonator losses. The corresponding external quality factor is characterized by the coupling capacitors to external circuitry. We note that resonator dephasing was not reported to play a major role in recent circuit QED experiments done with comparable resonators, in particular at low photon numbers.[45] In any case, the role of nonvanishing excess phase noise requires a separate, more detailed treatment with respect to an intended experimental realization of our setup.

B. Bloch-Redfield quantum master equation

The dissipative dynamics of the qubit-two-resonator system is obtained by tracing out the bath degrees of freedom of the total density operator $\varrho_{\rm tot}$ associated with the transformed system-bath Hamiltonian,

$$\mathcal{H}_{\rm tot} = \mathcal{H} + \sum_\mu Q_\mu \sum_j c_j^\mu (d_{j,\mu}^\dagger + d_{j,\mu}) + \sum_\mu \sum_j \hbar\omega_j^\mu \left(d_{j,\mu}^\dagger d_{j,\mu} + \frac{1}{2}\right), \tag{8}$$

where the qubit-bath coupling operators Q_x and Q_z are now written in the qubit eigenbasis according to Eq. (6). For weak system-bath interaction, the baths can be eliminated within Bloch-Redfield theory[46,47] as follows: Assuming that the baths are initially in thermal equilibrium at temperatures T_μ and not correlated with the system state ϱ, the total system-bath state can be written as $\varrho_{\rm tot}\propto\varrho\otimes\Pi_\mu\exp(-\Sigma_j\hbar\omega_j^\mu d_{j,\mu}^\dagger d_{j,\mu}/k_{\rm B}T_\mu)$. Then, one can derive within perturbation theory the quantum master equation for the reduced system density operator $\varrho=\mathrm{Tr}_{\rm bath}[\varrho_{\rm tot}]$. This procedure yields

$$\dot\varrho(t) = -\frac{i}{\hbar}[\mathcal{H},\varrho(t)] + \frac{1}{\hbar^2}\sum_\mu \int_0^\infty d\tau K_\mu(\tau) \times[\tilde Q_\mu(-\tau)\varrho(t)Q_\mu - Q_\mu\tilde Q_\mu(-\tau)\varrho(t)] + \mathrm{H.c.} \tag{9}$$

The environment correlation functions $K_\mu(\tau)$ are given by

$$K_\mu(\tau) = \frac{\hbar}{\pi}\int_0^\infty \mathrm{d}\omega J_\mu(\omega)\left[\coth\left(\frac{\hbar\omega}{2k_{\rm B}T_\mu}\right)\cos\,\omega\tau - i\,\sin\,\omega\tau\right], \tag{10}$$

where, $J_\mu(\omega)$ are the spectral densities (7). The Heisenberg operators $\tilde Q_\mu(\tau)=U_0^\dagger(\tau)Q_\mu U_0(\tau)$ are constructed via the system propagator $U_0(\tau)=\mathcal{T}[\exp\{-(i/\hbar)\int_0^\tau dt\mathcal{H}(t)\}]$. Here, the time ordering operator $\mathcal{T}$ is only required for an explicitly time-dependent system Hamiltonian.

We note that Eq. (9) is based on a Born-Markov approximation, since the bath correlation functions are supposed to decay sufficiently fast as compared to typical time scales of intrinsic system evolution. Thus, it was appropriate to extend the integral in Eq. (9) to infinity. Consistently, we assume Ohmic spectral densities in the correlation functions of Eq. (10), modeling $Z(\omega)$ as an effective resistance. However, this restriction is only necessary in the low-frequency region of the qubit environments. There, we assume

$$J_\mu(\omega) = \alpha_\mu\omega \quad \mu\in\{x,z\},\ \ \omega\ll\omega_{\rm qb}, \tag{11}$$

and the coefficients α_μ represent the dimensionless damping strengths. As we will see later, in the high-frequency regime, we are interested only in infinitely small intervals around frequencies such as $\omega_{\rm qb}$, Ω_A, and Ω_B. Hence, the Born-Markov approximation remains justified by expanding $J_\mu(\omega)$ to first order in these intervals. In this way, the only remaining restriction is that $J_\mu(\omega)$ is a smooth function around the frequencies of relevance. Within the scope of this work, we shall consider Eqs. (9)–(11) as a full description of the influence of dissipation and decoherence on the two-resonator setup.

This reasoning excludes in particular $1/f$ noise, which affects the phase coherence of superconducting qubits[31,33,48] due to its high impact at low frequencies. One typically describes $1/f$ noise by calculating the accumulated random phase as a function of time for specific experimental

protocols.[32,48,49] However, as shown below, we expect the effect of qubit dephasing to be suppressed even more than relaxation effects in the setup described here.

Since the quantum master equation (9) is nontrivial with respect to analytical treatment, we only use it for numerical purposes. However, in Sec. III, we derive a simplified effective quantum master equation in the dispersive regime, which will allow for analytic insight into the dissipative behavior of the two-resonator circuit.

C. Qubit decay rates

So far, we have modeled the coupling of the qubit to the baths in the laboratory frame. In this way, we can include the relevant noise channels for any particular qubit architecture into our formalism easily. However, with regard to physical understanding, it is more favorable to work in the qubit energy eigenframe and refer to what is commonly called energy relaxation and pure dephasing. The former describes bath-induced level transitions, while the latter accounts for the pure loss of phase coherence without a change of the system energy. In order to define the decay rates corresponding to these two processes, we first review the dissipation mechanisms of the qubit alone. To this end, we derive the quantum master equation describing the evolution of the reduced qubit density matrix $\varrho_{\rm qb}$ for a single qubit associated with the Hamiltonian $\mathcal{H}_{\rm qb}=\hbar\omega_{\rm qb}\sigma_z/2$ in the energy eigenbasis. Using the formalism detailed in Appendix A, we find

$$\dot{\varrho}_{\rm qb}(t) = -\frac{i}{\hbar}[\mathcal{H}_{\rm qb},\varrho_{\rm qb}(t)] + \gamma(\omega_{\rm qb})\left\{\sigma^-\varrho_{\rm qb}(t)\sigma^+ - \frac{1}{2}[\sigma^+\sigma^-,\varrho_{\rm qb}(t)]_+\right\} + \gamma_\phi(\omega\to 0)[\sigma_z\varrho_{\rm qb}(t)\sigma_z - \varrho_{\rm qb}(t)], \tag{12}$$

where $[\mathcal{A},\mathcal{B}]_+=\mathcal{A}\mathcal{B}+\mathcal{B}\mathcal{A}$ denotes the anticommutator between the operators $\mathcal{A}$ and $\mathcal{B}$. The dissipator in the third line of Eq. (12) does not affect the populations of the qubit eigenstates, but only accounts for the decay of the off-diagonal elements of the density operator. Thus, the rate $\gamma_\phi(\omega\to 0)$ can be associated with pure dephasing. The dissipator in the second line of Eq. (12) induces transitions between the qubit eigenstates, hence $\gamma(\omega_{\rm qb})$ characterizes relaxation. Assuming an overall temperature $T=T_x=T_z$, and following Eqs. (A7) and (A9), the qubit energy relaxation rate $\gamma(\omega_{\rm qb})$ and pure dephasing rate $\gamma_\phi(\omega\to 0)$ are obtained as

$$\gamma(\omega_{\rm qb}) = J_x(\omega_{\rm qb})\cos^2\theta + J_z(\omega_{\rm qb})\sin^2\theta, \tag{13}$$

$$\gamma_\phi(\omega\to 0) = \frac{k_{\rm B}T}{\hbar}(\alpha_z\cos^2\theta + \alpha_x\sin^2\theta). \tag{14}$$

Equations (13) and (14) link the physical system-bath interactions quantified in the laboratory frame to the pure bit-flip and dephasing mechanisms relevant in the qubit eigenbasis. Moreover, they highlight the dependence of the pure decay rates on the applied flux in terms of the mixing angle θ. In particular, for a flux qubit, flux noise can be responsible for both relaxation and dephasing. We emphasize that, in this special scenario, $J_x(\omega)=0$ and $J_z(\omega)\neq 0$, and Eq. (13) is consistent with results from other works.[32,48,49]

III. ANALYTICAL TREATMENT OF DECOHERENCE IN THE DISPERSIVE LIMIT

In the setup of Fig. 1, the qubit can mediate a controllable coupling between the two resonators, i.e., it can act as a quantum switch between them. In this section, we review the quantum switch Hamiltonian of Ref. 27 and extend it beyond the rotating-wave approximation. Furthermore, we derive an effective quantum master equation which allows us to understand by purely analytical arguments that the quantum switch is affected by the qubit dissipation only in second (relaxation) and fourth order (dephasing), respectively.

A. Dispersive Hamiltonian within the rotating-wave approximation: The quantum switch

In order to function as a quantum switch, the two-resonator circuit must be operated in the dispersive limit, where the qubit-resonator detuning Δ is large as compared to the qubit-oscillator coupling,

$$g \ll \Delta, \quad \Delta = \omega_{\rm qb} - \Omega, \tag{15}$$

and the parameter λ_Δ is necessarily small,

$$\lambda_\Delta = \frac{g\sin\theta}{\Delta}, \quad |\lambda_\Delta| \ll 1. \tag{16}$$

Here and henceforth, we confine ourselves to symmetric setups with $\Omega=\Omega_{\{A,B\}}$ and $g=g_{\{A,B\}}$. This is not expected to be a serious restriction in practice, though.[27]

In the dispersive limit determined by Eq. (15), the Hamiltonian of Eq. (5) can be diagonalized approximately. To this end, it is first simplified with a rotating-wave approximation as follows. Writing $\sigma_x=\sigma^+ + \sigma^-$ with the fermionic raising and lowering operators $\sigma^+=|e\rangle\langle g|$ and $\sigma^-=|g\rangle\langle e|$, one can move to the interaction picture with respect to the uncoupled Hamiltonian. Then, the coupling operators σ^+a, $\sigma^-a^\dagger$, σ^+b, and $\sigma^-b^\dagger$ oscillate with the phase factors $\exp[\pm i\Delta t]$, whereas σ^-a, $\sigma^+a^\dagger$, σ^-b, and $\sigma^+b^\dagger$ oscillate with $\exp[\pm i\Sigma t]$, where

$$\Sigma = \Omega + \omega_{\rm qb}. \tag{17}$$

Close to resonance, the resonator-qubit detuning is small and, consequently, $|\Delta|\ll\Sigma$. Thus, the former set of operators oscillates slowly, whereas the latter exhibit fast "counter-rotating" oscillations. For sufficiently weak coupling $g \ll \min\{\omega_{\rm qb},\Omega\}$, one can separate time scales and average the counter-rotating terms to zero. In this way, the first-order interaction Hamiltonian between qubit and resonators is Jaynes-Cummings-like[50] and we describe our system with

$$\mathcal{H}^{\rm RWA} = \frac{\hbar\omega_{\rm qb}}{2}\sigma_z + \hbar\Omega a^\dagger a + \hbar\Omega b^\dagger b - \hbar\Delta\lambda_\Delta(\sigma^+a + \sigma^-a^\dagger + \sigma^+b + \sigma^-b^\dagger) + \hbar G(a^\dagger b + ab^\dagger). \tag{18}$$

In a second step, we apply the unitary transformation $\mathcal{U}^{\rm RWA}=\exp(-\lambda_\Delta\mathcal{D})$, where

$$\mathcal{D} = \sigma^- a^\dagger - \sigma^+ a + \sigma^- b^\dagger - \sigma^+ b. \tag{19}$$

Finally, we truncate the transformed Hamiltonian $\mathcal{H}_{\mathrm{eff}}^{\mathrm{RWA}} = \mathcal{U}_{\mathrm{RWA}}^\dagger \mathcal{H}^{\mathrm{RWA}} \mathcal{U}_{\mathrm{RWA}}$ to second order in λ_Δ, yielding

$$\mathcal{H}_{\mathrm{eff}}^{\mathrm{RWA}} = \hbar\Omega(a^\dagger a + b^\dagger b + 1) + \frac{\hbar\omega_{\mathrm{qb}}}{2}\sigma_z + \hbar\Delta\lambda_\Delta^2\sigma_z(a^\dagger a + b^\dagger b + 1) + \hbar\hat{g}_{\mathrm{SW}}^{\mathrm{RWA}}(ab^\dagger + a^\dagger b). \tag{20}$$

Here, the first line describes qubit and resonators, the second ac-Stark/Zeeman and Lamb shifts, and the third an effective coupling between the two resonators. The corresponding coupling operator is

$$\hat{g}_{\mathrm{SW}}^{\mathrm{RWA}} = G + \Delta\lambda_\Delta^2\sigma_z. \tag{21}$$

A remarkable feature of the Hamiltonian of Eq. (20) is that it commutes with σ_z, i.e., $[\mathcal{H}_{\mathrm{eff}}^{\mathrm{RWA}}, \sigma_z] = 0$. Consequently, the qubit state will not change during the unitary evolution of the system. When the qubit is prepared in a suitable eigenstate, it can be traced out. Throughout this work, we consider the qubit to be initially prepared in its ground state $|g\rangle\langle g|$. Then, $\hat{g}_{\mathrm{SW}}$ simplifies to the resonator-resonator coupling constant

$$g_{\mathrm{SW}}^{\mathrm{RWA}} = G - \lambda_\Delta^2\Delta. \tag{22}$$

In this case, the Hamiltonian of Eq. (20) describes two coupled harmonic oscillators. By means of either adiabatic or oscillating external flux signals, the qubit can be tuned such that the interaction between the resonators is either switched on ($|g_{\mathrm{SW}}^{\mathrm{RWA}}| \neq 0$) or off ($|g_{\mathrm{SW}}^{\mathrm{RWA}}| = 0$). This feature is referred to as the switch-setting condition. With the help of specific protocols, it can be utilized to create entangled states out of initial bi-resonator product states.

We note that the effective coupling between both resonators can be interpreted as a beam-splitter interaction. A comparable quantum-optical setup was proposed in Ref. 51. There, an atom passing through a cavity serves to create entanglement between two optical fields inside the cavity. That system is described by an effective Hamiltonian quite analogous to Eq. (20).

For this work the "adiabatic" shift protocol is of particular relevance. There, parameters are initially chosen so as to fulfill the switch-setting condition when the qubit is in $|g\rangle$. Then, the resonator-resonator interaction can be turned on by adiabatically varying the flux bias. Experiments have shown that a flux change slow enough to avoid significant population of the excited state can be realized easily even in pulsed setups.[32]

Regarding the influence of a dissipative environment on the quantum switch, we already note that, for suitable switching protocols and at sufficiently low temperatures, the qubit energy relaxation and dephasing will not affect the operation of the switch in first order. As one of the main results of this work, we give analytic arguments to put this statement on firm theoretical footings in Sec. III C.

B. Dispersive Hamiltonian beyond the rotating-wave approximation

In the process of deriving Eq. (20) in the previous section, a rotating-wave approximation is applied to the Hamiltonian (5) at the level of first-order in the qubit-oscillator coupling. However, it has recently been revealed that neglecting the counter-rotating terms may lead to inaccuracies.[52] Especially in the case of far detuning described by Eq. (15), the rotating-wave approximation causes noticeable deviations from results obtained numerically from the full Hamiltonian of Eq. (5) for typical parameters. Nevertheless, the effective, dispersive Hamiltonian can be obtained by means of the unitary transformation

$$\mathcal{U} = \exp(-\lambda_\Delta\mathcal{D} - \lambda_\Sigma\mathcal{S} - \lambda_\Omega\mathcal{W}). \tag{23}$$

Here,

$$\mathcal{S} = \sigma^- a - \sigma^+ a^\dagger + \sigma^- b - \sigma^+ b^\dagger, \tag{24}$$

$$\mathcal{W} = \sigma_z(a - a^\dagger) + \sigma_z(b - b^\dagger), \tag{25}$$

and the corresponding coefficients are

$$\lambda_\Sigma = \frac{g\sin\theta}{\Sigma}, \quad |\lambda_\Sigma| \ll 1, \tag{26}$$

$$\lambda_\Omega = \frac{g\cos\theta}{\Omega}, \quad |\lambda_\Omega| \ll 1. \tag{27}$$

The above inequalities allow us to discard terms of orders higher than $\lambda_{\{\Delta,\Sigma,\Omega\}}^2$ when computing the effective second-order Hamiltonian $\mathcal{H}_{\mathrm{eff}} = \mathcal{U}^\dagger\mathcal{H}\mathcal{U}$. In this case,

$$\mathcal{H}_{\mathrm{eff}} = \hbar\Omega(a^\dagger a + b^\dagger b + 1) + \frac{\hbar\omega_{\mathrm{qb}}}{2}\sigma_z + \hbar(\Delta\lambda_\Delta^2 + \Sigma\lambda_\Sigma^2)\sigma_z(a^\dagger a + b^\dagger b + 1) + \hbar\hat{g}_{\mathrm{SW}}(ab^\dagger + a^\dagger b) \tag{28}$$

becomes diagonal. In the above equation, we use the qubit-state-dependent resonator-resonator coupling operator

$$\hat{g}_{\mathrm{SW}} = G + (\lambda_\Delta^2\Delta + \lambda_\Sigma^2\Sigma)\sigma_z. \tag{29}$$

At this point, we can gain insight about the effect of the transformation $\mathcal{U}$ [Eq. (23)] on the Hamiltonian. We first note that, when applying the rotating-wave approximation to $\mathcal{H}$, only the exponent $\mathcal{D}$ is required to produce a diagonal second-order Hamiltonian, cf. Sec. III A. Beyond this simple scenario,[52] the exponent $\mathcal{S}$ cancels the first-order counter-rotating terms of $\mathcal{H}$. Furthermore, the polaron transformation represented by the exponent $\mathcal{W}$ must be applied to eliminate off-diagonal interaction terms such as $g\cos\theta\sigma_z(a+a^\dagger)$, which cause qubit-state-dependent energy shifts of the oscillator coordinates when the qubit is biased away from its degeneracy point.

However, in $\mathcal{H}_{\mathrm{eff}}$, terms of the order $\lambda_{\{\Delta,\Sigma,\Omega\}}^2$, such as, e.g., $\sigma^+(a^{(\dagger)})^2$ or $\sigma^+ a^\dagger a$, need to be canceled with a rotating-wave argument. We emphasize that this rotating-wave approximation in second order in $\mathcal{H}_{\mathrm{eff}}$ still allows for an accurate description of our system in the dispersive regime, whereas a

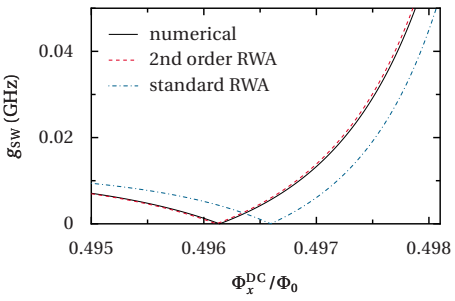

FIG. 2. (Color online) Switch setting coefficient g_{SW} (qubit in the ground state) for the RWA (blue dash-dotted line) and non-RWA case, Eq. (30) (red dashed line), compared to numerical data obtained from the diagonalization of Hamiltonian (1) (black solid line). All quantities are plotted against the qubit flux bias Φ_x^{DC}. Parameters are $\Omega/2\pi=3.5$ GHz, $\delta_Q/2\pi=4$ GHz, $G/2\pi=0.0022$ GHz, and $g/2\pi=0.24$ GHz.

rotating-wave approximation in the first-order Hamiltonian $\mathcal{H}$ does not. Following the same reasoning, we may also neglect terms $\propto G/\Delta, G/\Sigma, \ldots \ll 1$. The effective Hamiltonian $\mathcal{H}_{\text{eff}}$ of Eq. (28) has the same structure as its rotating-wave counterpart $\mathcal{H}_{\text{eff}}^{\text{RWA}}$ of Eq. (20). However, there is one important quantitative difference: the detuning dependence $\lambda_\Delta^2\Delta$ of the coupling coefficients is replaced by the expression $(\lambda_\Delta^2\Delta+\lambda_\Sigma^2\Sigma)$. In particular, the effective resonator-resonator coupling constant is

$$g_{\text{SW}} = G - (\lambda_\Delta^2\Delta + \lambda_\Sigma^2\Sigma) \tag{30}$$

for the qubit being in its ground state. The effect of the counter-rotating terms is visualized in Fig. 2. There, we compare $g_{\text{SW}}^{\text{RWA}}$ and g_{SW} to the numerically exact coupling coefficient for adequate parameters. Obviously, in contrast to $g_{\text{SW}}^{\text{RWA}}$, the agreement is excellent for g_{SW}. This finding once more confirms the necessity to include counter-rotating terms of first order in the qubit-oscillator coupling in the full system Hamiltonian. It also confirms the validity of the rotating-wave approximation in second order of $\lambda_{\{\Delta,\Sigma,\Omega\}}$ applied to the dispersive Hamiltonian. We also illustrate the importance of the non-RWA features below, where we develop a dissipative description of the quantum switch Hamiltonian coupled to different reservoirs.

C. Effective master equation for the quantum switch setup

In this section, we analytically investigate the dissipative behavior of the two-resonator-qubit system. To this end, we derive an effective quantum master equation for the reduced density matrix of our system in the dispersive limit.[53,54] In particular, we study the additional dissipation imposed on the resonators due to the presence of the qubit.

In principle, we combine the procedure explained in Sec. III B with that of Sec. II C and apply it to the system-bath Hamiltonian $\mathcal{H}_{\text{tot}}$ of Eq. (5), which includes all counter-rotating terms. First, we compute the total dispersive Hamiltonian $\mathcal{H}_{\text{tot,eff}}=\mathcal{U}^\dagger\mathcal{H}_{\text{tot}}\mathcal{U}$ using the transformation (23) and truncate it to second order with respect to the parameters $\lambda_{\{\Delta,\Sigma,\Omega\}}$, as described above. During this procedure, we obtain the effective system-bath coupling operators

$$Q_{\mu,\text{eff}} = \mathcal{U}^\dagger Q_\mu \mathcal{U}, \quad \mu \in \{A,B,x,z\}. \tag{31}$$

The explicit expressions for these effective coupling operators are given in Appendix B. In the next step, we derive the effective quantum master equation following the lines of Refs. 55 and 56. While the interested reader can find the details in Appendix C, we give a short summary of the most important steps in the following. Motivated by the usual experimental conditions in circuit QED, we assume an equal temperature for all baths, $T=T_{\{x,z,A,B\}}$, and confine ourselves to the low-temperature regime $k_BT/\hbar \ll \min\{\omega_{\text{qb}},\Delta,\Omega,\Sigma\}$. Consequently, we neglect all contributions to the dissipative system dynamics that describe energy absorption from the baths.

Using Eq. (9) as a starting point, we move first to an interaction picture with respect to the uncoupled qubit and resonators and insert the spectral decompositions of the effective coupling operators. In the following, we perform a semisecular approximation.[56] To this end, we dismiss terms that evolve rapidly compared to the time evolution of the system state, i.e., on system time scales $\{\Omega,\omega_{\text{qb}},\Delta,\Sigma\}^{-1}$. On the contrary, we keep those terms that oscillate slowly at frequencies such as $\lambda_\Delta^2\Delta, \lambda_\Sigma^2\Sigma, \lambda_\Omega^2\Omega$. We emphasize that our result goes beyond the standard Lindblad master equation, where one would perform a full secular approximation, dismissing all oscillating contributions. In this way, we obtain the effective quantum master equation for the reduced system state, Eq. (C17). There, we assume $\alpha_{\{x,z\}} \ll \hbar\omega_{\text{qb}}/k_BT$ in order not to violate the Markov approximation.

In order to gain physical insight into the influence of dissipation on the quantum switch setup, we can simplify the complicated effective master equation of Eq. (C17). In the dispersive regime, the qubit mediates part of the coupling between the resonators by exchanging virtual, but not real excitations with them. In particular, as discussed in Sec. III B, the switch can be operated in a way that the qubit is initially prepared in the ground state and remains there during the whole time evolution, as it cannot suffer from further decoherence. In this scenario, the qubit degrees of freedom can be traced out and the reduced Hamiltonian of the coupled resonators becomes

$$\mathcal{H}_{\text{cav}}^{\text{eff}} = \hbar\Omega(a^\dagger a + b^\dagger b + 1) - \hbar(\lambda_\Delta^2\Delta + \lambda_\Sigma^2\Sigma)(a^\dagger a + b^\dagger b + 1) + \hbar g_{\text{SW}}(ab^\dagger + a^\dagger b). \tag{32}$$

With the dissipator $\mathcal{D}[X]$ acting on an operator X in the product Hilbert space of the resonators,

$$\mathcal{D}[X]\varrho_{\text{cav}} = X\varrho_{\text{cav}}X^\dagger - \frac{1}{2}[X^\dagger X, \varrho_{\text{cav}}]_+, \tag{33}$$

we can write down the effective Lindblad-type quantum master equation for the reduced state ϱ_{cav} of the two coupled oscillators up to second order in λ_Δ and λ_Σ,

$$\dot{\varrho}_{\text{cav}} = -\frac{i}{\hbar}[\mathcal{H}_{\text{cav}}^{\text{eff}}, \varrho_{\text{cav}}] + \kappa_A\mathcal{D}[a]\varrho_{\text{cav}} + \kappa_B\mathcal{D}[b]\varrho_{\text{cav}} + \kappa_{\text{qb}}\mathcal{D}[a+b]\varrho_{\text{cav}}. \tag{34}$$

The above equation reveals the relevant processes governing

the dissipative behavior of the quantum switch. The dissipators $\mathcal{D}[a]$ and $\mathcal{D}[b]$ represent the independent decay channels due to the individual environments of the resonators A and B, respectively. The corresponding decay rates are the inverse lifetimes of the uncoupled resonators, $\kappa_A = J_A(\Omega)$ and $\kappa_B = J_B(\Omega)$. These rates may incorporate the combined effects of internal and external loss mechanisms, according to the discussion in Sec. II A. In addition to these contributions, the qubit introduces extra dissipation on the resonators via the dissipator $\mathcal{D}[a+b]$. The appearance of the center-of-mass coordinate $a+b$ of the two-resonator system in the dissipator originates from the system Hamiltonian of Eq. (5), where the qubit couples to the resonator "center of mass" coordinate, i.e., the interaction is proportional to $\sigma_x(a+b+a^\dagger+b^\dagger)$ and $\sigma_z(a+b+a^\dagger+b^\dagger)$, respectively. The qubit-induced damping rate is

$$\kappa_{\mathrm{qb}} = (\lambda_\Delta + \lambda_\Sigma)^2 (J_x(\Omega)\cos^2\theta + J_z(\Omega)\sin^2\theta) = (\lambda_\Delta + \lambda_\Sigma)^2 \gamma(\Omega), \tag{35}$$

where $\gamma(\Omega)$ is the rate defined in Eq. (A7) for the bare qubit. In the expressions for κ_A, κ_B, and κ_{qb}, the spectral densities $J_{\{A,B,x,z\}}(\omega)$ are required to be smooth functions at $\omega=\Omega$ in order that Ohmic behavior can be assumed locally. The reasoning is the same as the one presented in Appendix A.

The qubit-induced damping rate of the two-resonator system, κ_{qb} of Eq. (35), constitutes one central result of this work and has several remarkable features. First of all, we note that $\gamma(\Omega)$ has the same functional dependence on the qubit mixing angle θ as the relaxation rate $\gamma(\omega_{\mathrm{qb}})$ of the bare qubit, Eq. (13). However, $J_{\{A,B,x,z\}}(\Omega)$ and the corresponding $J_{\{A,B,x,z\}}(\omega_{\mathrm{qb}})$ are not necessarily equal, thus the values of both rates are different in general. Second, the rate κ_{qb} is of second order in λ_Δ and λ_Σ because the qubit-mediated interaction responsible for the effective noise channel in Eq. (34) is a second-order effect. This also explains the, at a first glance, surprising fact that the qubit induces a decay of the two-resonator system even though its excited state is never populated. We can understand this by recalling that the resonator-resonator interaction is mediated not by real, but by virtual qubit excitations, which are known to give rise to second-order effects. Equivalently, we may apply a more classical picture, which is based on the fact that the resonator-resonator coupling coefficient g_{SW} of Eq. (30) depends on the qubit-resonator detuning. Hence, the qubit baths, which cause first-order fluctuations to the qubit level splitting, induce second-order fluctuations of g_{SW}. The latter are described by the last term of Eq. (34).

Remarkably, the associated decay rate κ_{qb} is related to the qubit relaxation γ, whereas dephasing γ_ϕ would enter the effective master equation (34) only in fourth order in $\lambda_{\{\Delta,\Sigma\}}$ [cf. also Eq. (C17)]. Mathematically, this can be understood from the structure of the dispersive operator $\sigma_{z,\mathrm{eff}}$ of Eq. (B5), which couples the system to dephasing noise. To the order $\lambda_{\{\Delta,\Sigma\}}$, this operator contains products of operators which change the populations of the qubit and resonators simultaneously. On the one hand, the term $\sigma^+ a$, for example, describes the excitation of the qubit together with the emission of a resonator photon, a process which is energetically forbidden at low temperatures for $\Delta=\omega_{\mathrm{qb}}-\Omega>0$. On the other hand, terms such as $\sigma^- a^\dagger$ and $\sigma^- b^\dagger$ have no effect when the qubit remains in the ground state. By contrast, the operator $\sigma_{x,\mathrm{eff}}$ of Eq. (B4), which is responsible for the qubit energy relaxation, contains terms such as $\sigma_z(a+b)$ of the order $\lambda_{\{\Delta,\Sigma\}}$. These describe a resonator decay without exciting the qubit, which is energetically favorable at low temperatures. For this reason, the only remaining contribution to qubit-enhanced decay up to second order in $\lambda_{\{\Delta,\Sigma\}}$ in the effective quantum master equation for the two resonators, Eq. (34), stems from qubit relaxation. The fourth-order contribution to the dephasing is related to the appearance of corresponding operators of the order $\lambda^2_{\{\Delta,\Sigma\}}$ in $\sigma_{z,\mathrm{eff}}$, which change the states of the resonators but not that of the qubit.

IV. NUMERICAL RESULTS

We now investigate the validity of the effective Hamiltonian (28) with respect to the resonator-resonator coupling constant, Eq. (29) and the effective quantum master equation (34) for the resonators. Therefore, we compare the analytical results derived in the previous sections to numerically exact results obtained with the Bloch-Redfield quantum master equation (9) using the full Hamiltonian (5). For further convenience, we assume uniform resonator decay rates, $\kappa=\kappa_A=\kappa_B$. In our numerical simulations we use conservative estimates for the qubit decay rates. This is to stress the effect of the qubit dissipation channel on the resonators.

A. Rabi oscillations

The observation of Rabi oscillations between the two resonators is a first feasible application to probe the two-resonator setup. A system prepared in the product state $|g\rangle_{\mathrm{qb}}|1\rangle_A|0\rangle_B$ is subject to a periodic exchange of the excitation between the resonators as long as their coupling is finite, $g_{\mathrm{SW}}\neq 0$. The corresponding oscillation time is $T_{\mathrm{Rabi}}=\pi/g_{\mathrm{SW}}$. The initial excitation could be provided to one of the resonators by means of an ancilla qubit. For this purpose, suitable protocols have recently been proposed.[22,57–59]

Figure 3(a) depicts the according behavior of the resonator populations as a function of time. We find the numerically observed oscillation period to be in good agreement to T_{Rabi}. Note that we have already incorporated the effects of the dissipative environments modeled by the Bloch-Redfield master equation (9) (see discussions in the following sections). The time evolution of the qubit population $\langle\sigma_z\rangle$ is plotted in Fig. 3(b). From this we can verify that the qubit remains in its ground state after weak initial transients. These findings substantiate the validity of the effective Hamiltonian (28) in the dispersive regime.

B. Decay rates

In the following we are interested in understanding quantitatively the influence of the reservoirs on the two-resonator setup. For this purpose we first make an analytical estimation based on the effective quantum master equation (34), which are compared then to numerical results obtained with Eq. (9). We investigate the time evolution of particular observables,

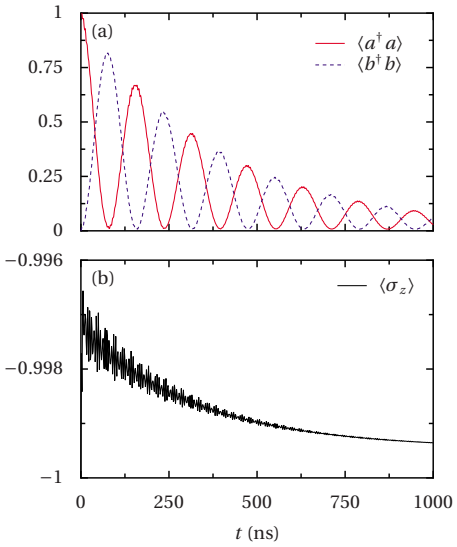

FIG. 3. (Color online) (a) Rabi oscillations between the resonators at the effective interaction strength $g_{\mathrm{GSW}}/2\pi=0.00315$ GHz (numerical value, analytically we find $g_{\mathrm{GSW}}/2\pi=0.00328$ GHz): Occupation numbers of resonator A (solid red lines) and B (dashed blue lines). The initial state is $|g\rangle_{\mathrm{qb}}|1\rangle_A|0\rangle_B$. (b) Time evolution of the qubit state in terms of $\langle\sigma_z\rangle$ (solid black lines). The deviation from the ground state always lies below 0.5%. Numerical parameters: $\Omega/2\pi=3.5$ GHz, $\delta_Q/2\pi=4$ GHz, $\varepsilon/2\pi=-6.37$ GHz, $g/2\pi=0.24$ GHz, $G/2\pi=0.0022$ GHz, $T=20$ mK. Decay rates: $J_A(\Omega)/2\pi=J_B(\Omega)/2\pi=0.00035$ GHz, $J_x(\Omega)/2\pi=J_z(\Omega)/2\pi=0.035$ GHz.

the associated operators of which are constants of motion with respect to the dynamics of the closed system. Thus, any dynamics is produced by the dissipators of the quantum master Eqs. (9) or (34), respectively.

At this point we recall that the effective Hamiltonian simply describes a set of two coupled harmonic oscillators as long as the qubit remains in its ground state. They are each coupled to independent noise channels, as well as to a joint channel of qubit-induced correlated noise via their "center of mass coordinate." The latter is defined as the bosonic operator $A_+=(a+b)/\sqrt{2}$. In addition we define the "relative coordinate" $A_-=(a-b)/\sqrt{2}$. In terms of these normal modes the oscillators are not coupled. The associated number operators are constants of motion, $[\mathcal{H}_{\mathrm{eff}},A_\pm^\dagger A_\pm]=0$. For further progress we compute the time evolution of the averages $\langle A_\pm^\dagger A_\pm\rangle$ using the effective quantum master equation for the two-resonator system (34). Here we note that the evolution of any operator $\mathcal{O}$ without explicit time dependence is described by the adjoint of the quantum master equation (34),

$$\partial_t\langle\mathcal{O}\rangle=\frac{i}{\hbar}\langle[\mathcal{H}_{\mathrm{cav}}^{\mathrm{eff}},\mathcal{O}]\rangle+\kappa\langle D^\dagger[a]\mathcal{O}\rangle+\kappa\langle D^\dagger[b]\mathcal{O}\rangle+\kappa_{\mathrm{qb}}\langle D^\dagger[a+b]\mathcal{O}\rangle, \tag{36}$$

with

$$\partial_t\langle\mathcal{O}\rangle=\mathrm{tr}(\partial_t\rho\mathcal{O}).$$

The adjoint Lindblad superoperators $D^\dagger$ act on the operator $\mathcal{O}$, according to

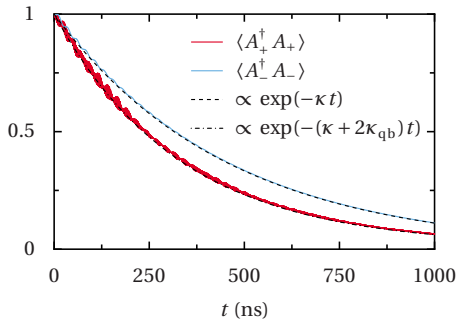

FIG. 4. (Color online) Decay of the quantum switch out of the initial state $|g\rangle_{\mathrm{qb}}|1\rangle_A|0\rangle_B$. Numerical data obtained with the Bloch-Redfield QME (9) and $N=3$ states in each resonator: Decay of the expectation values of the number operators corresponding to the "center of mass coordinate", $\langle A_+^\dagger A_+\rangle$ (red solid lines, thicker curve) and "relative coordinate", $\langle A_-^\dagger A_-\rangle$ (blue solid lines, thinner curve), compared to analytical estimates, Eqs. (38) and (39) (black dashed and dash-dotted lines, respectively). Decay rates are according to Eq. (34). Parameters: see Fig. 3.

$$D^\dagger[X]\mathcal{O}=X^\dagger\mathcal{O}X-\frac{1}{2}[X^\dagger X,\mathcal{O}]_+, \tag{37}$$

cf. Eq. (33). Evaluating this relation for the normal mode number operators $\mathcal{O}=A_\pm^\dagger A_\pm$ yields

$$\langle A_+^\dagger A_+\rangle(t)=\langle A_+^\dagger A_+\rangle_{t=0}e^{-(\kappa+2\kappa_{\mathrm{qb}})t} \tag{38}$$

and

$$\langle A_-^\dagger A_-\rangle(t)=\langle A_-^\dagger A_-\rangle_{t=0}e^{-\kappa t}. \tag{39}$$

The normal modes are thus expected to decay exponentially. Remarkably, these decays should occur at different rates. The qubit-induced noise channel only couples to the center of mass, which suffers enhanced decay. This becomes manifest in the contribution $2\kappa_{\mathrm{qb}}$ to the exponent in Eq. (38), with the rate κ_{qb} from Eq. (35). The relative coordinate is not affected by the qubit noise channel, however, and simply decays with the resonator decay rate κ, see Eq. (39). Formally, this is because of

$$D^\dagger[a+b]A_-^\dagger A_-=0.$$

In order to test these analytical estimations based on Eq. (34), we consider a decay scenario with the resonators initially prepared in the Fock states $|1\rangle_A$ (resonator A) and $|0\rangle_B$ (resonator B). The qubit is prepared in its ground state $|g\rangle_{\mathrm{qb}}$. We calculate numerically the time evolution of the number operators related to the "center of mass," $\langle A_+^\dagger A_+\rangle$, and the "relative coordinate," $\langle A_-^\dagger A_-\rangle$, and compare the decay characteristics to the ones suggested by Eqs. (38) and (39), respectively. The results are depicted in Fig. 4 for a particular set of parameters. We find an excellent agreement of theory and numerical data. While $\langle A_-^\dagger A_-\rangle$ decays at a rate κ, the decay of $\langle A_+^\dagger A_+\rangle$ is enhanced by the qubit noise channel, resulting in a decay rate $\kappa+2\kappa_{\mathrm{qb}}$. The latter finding is affirmed in Fig. 5(b), where we compare the analytical expression for the decay rate $\kappa+2\kappa_{\mathrm{qb}}$ to corresponding numerical values that are extracted from simulations of a decay scenario according to Eq. (38). The qubit-induced decay rate κ_{qb}

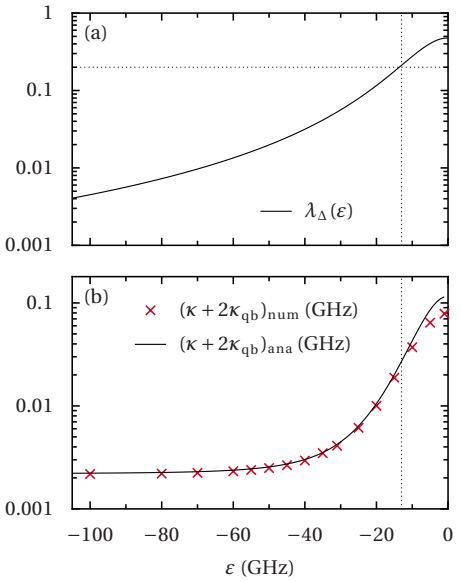

FIG. 5. (Color online) Dependence of the parameter λ_Δ (a) and the effective damping rate $\kappa+2\kappa_{qb}$ (b) (black solid lines), on the qubit energy bias ε. The rate for qubit-enhanced decay κ_{qb} is given by Eq. (35). The numerically extracted damping rates [red crosses in (b)] are related to the decay of the expectation value of the number operator corresponding to the "center of mass coordinate", $\langle A_+^\dagger A_+\rangle$, out of the initial state $|g\rangle_{qb}|1\rangle_A|0\rangle_B$ at different ε. The dotted lines mark the limit of validity of the dispersive theory (see text). Parameters are chosen as in Fig. 3.

is given by Eq. (35). Here, we have chosen an explicit dependence on the qubit bias energy ε, which is adjustable in realistic experimental scenarios, while all other parameters are usually fixed. As indicated by Fig. 5(a), the dispersive description can be considered as valid for $\lambda_{\{\Delta,\Sigma,\Omega\}} \lesssim 0.1$. These findings suggest that the effective quantum master equation for the two coupled resonators (34) describes the dissipative system behavior adequately in the dispersive limit.

Furthermore, the stationary value of $\langle A_+^\dagger A_+\rangle$ is found to be different from zero. This stems from a static energetic shift of the oscillator potential minima due to a small "effective force." The latter arises from the resonator-qubit coupling component $\Omega\lambda_\Omega(a+a^\dagger)\sigma_z$ in the full system Hamiltonian (5), which has been eliminated in the effective Hamiltonian (C17) by the transformation (25). The dependence between the original and transformed oscillator creators and annihilators can be expressed as $a^{(\dagger)} \to a^{(\dagger)} - \lambda_\Omega$. First of all, this shift explains strong oscillations with frequency Ω during the time evolution of the resonator states. In Fig. 4, their effect is visible, however they are not resolved. The equilibrium value of the resonator "center of mass" population is shifted according to

$$\langle A_+^\dagger A_+\rangle \to \langle A_+^\dagger A_+\rangle - 4\lambda_\Omega^2. \tag{40}$$

Following the same reasoning, the equilibrium value of $\langle A_-^\dagger A_-\rangle$ is zero.

As a second example, we consider the case of each resonator prepared in a coherent state, $|\alpha\rangle = e^{-|\alpha|^2}\sum_{n=0}^{\infty}\frac{\alpha^n}{\sqrt{n!}}|n\rangle$ with

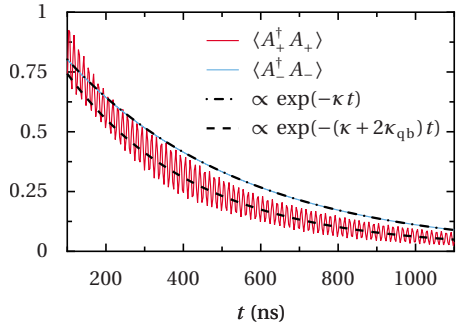

FIG. 6. (Color online) Decay of the quantum switch out of the initial coherent state $|\alpha\rangle$ with $\alpha=1$. Simulations were run with $N=6$ states in each resonator. Numerical data: occupations of the "center of mass coordinate", $\langle A_+^\dagger A_+\rangle$ (red solid lines, oscillating curve) and "relative coordinate", $\langle A_-^\dagger A_-\rangle$ (blue solid smooth line), compared to analytical estimates, Eqs. (38) and (39) (black dashed and dash-dotted lines, respectively). Initial transient effects are not depicted in the figure. Parameters: see Fig. 3.

$|\alpha|^2$ being the average photon number in the resonator. This scenario is mainly motivated by experiment, where a coherent state in a resonator can easily be prepared via a resonant drive. To investigate the decay behavior of the "center of mass" and "relative coordinate" for this scenario, we choose the initial state $|g\rangle_{qb}|\alpha=1\rangle_A|\beta=0\rangle_B$. As depicted in Fig. 6, the predictions of the effective quantum master equation are again found to be in good agreement with our numerical simulations, apart from transient effects.

C. Decay of entanglement

The generation of entangled two-resonator states is a key application of the quantum switch. For this purpose, we recall the switching property of the two-resonator setup mentioned in Sec. III B, that is, the possibility to switch on and off the effective coupling between the resonators by balancing the coupling coefficient g_{SW} given in Eq. (29). While a similar approach to create entanglement between two resonators based on Landau-Zener sweeps[60] has been previously discussed in Ref. 52, we focus on the following, suitable protocol: A finite interaction strength g_{SW}^{on} is initialized by tuning the qubit energy flux appropriately. After preparing the initial product state $|g\rangle_{qb}|1\rangle_A|0\rangle_B$ the two-resonator state $|\psi\rangle_{cav}$ evolves according to

$$|\psi(t)\rangle_{cav} = \cos(g_{SW}^{on}t)|1\rangle_A|0\rangle_B + i\,\sin(g_{SW}^{on}t)|0\rangle_A|1\rangle_B. \tag{41}$$

After a time $t=T_{on}$ has elapsed, g_{SW} is balanced back to zero. During the whole procedure the qubit remains in its ground state $|g\rangle_{qb}$ and does not get entangled with the resonators. In particular, $T_{on}=\pi/4g_{SW}$ results in the entangled two-resonator state $|\psi_+^i\rangle_{cav}=(|1\rangle_A|0\rangle_B+i|0\rangle_A|1\rangle_B)/\sqrt{2}$, whereas $T_{on}=3\pi/4g_{SW}^{on}$ yields the state $|\psi_-^i\rangle_{cav}=(|1\rangle_A|0\rangle_B - i|0\rangle_A|1\rangle_B)/\sqrt{2}$. A photon transfer from one resonator to the other is accomplished with $T_{on}=\pi/2g_{SW}^{on}$.

In the above discussions we have disregarded decoherence for reasons of clarification. In realistic scenarios, however, dissipation and dephasing are present even in the case of short times T_{on}, which prevents the creation of perfectly

entangled states according to the above described protocol. Beyond that, two-resonator entanglement once created, will decay with time, according to the effective two-resonator QME (34). In this context, excess phase noise in the resonators may cause further adverse effects, which are not considered here (cf. Sec. II A). Thus, it is important to reveal the decay characteristics of particular entangled states that could be created in the two-resonator setup up to a good degree via specific switch-setting protocols. For this purpose, we first focus on the decay characteristics of the initial entangled two-resonator Bell states

$$|\psi_{\pm}\rangle_{\mathrm{cav}} = \frac{1}{\sqrt{2}}[|1\rangle_A|0\rangle_B \pm |0\rangle_A|1\rangle_B]. \tag{42}$$

To quantify the entanglement we first assume that all dynamics is restricted to the subspace $\{|00\rangle,|01\rangle,|10\rangle,|11\rangle\}$. Thus, we face the dynamics of entanglement between two two-level systems. In this case, the concurrence C represents an adequate measure of entanglement, given by[61] $C=\max\{\xi_1-\xi_2-\xi_3-\xi_4,0\}$. The parameters ξ_j denote the ordered square roots of the eigenvalues of the matrix $\rho_{\mathrm{cav}}(\sigma_y^A\sigma_y^B)\rho_{\mathrm{cav}}^*(\sigma_y^A\sigma_y^B)$ with ρ_{cav} being the reduced density matrix of the two-resonator state, and A and B labeling the respective resonator Hilbert spaces. This representation of the concurrence is quite general and suitable for numerical investigation. However, for the initial states $|\psi_{\pm}\rangle_{\mathrm{cav}}$ and linear superpositions hereof, one can obtain analytical expressions for the decay characteristics of the concurrence with the help of the effective quantum master equation (34). Since the only nonzero elements of the associated density matrices during the whole time evolution are ρ_{00}, ρ_{11}, ρ_{22} and ρ_{12}, ρ_{21} in the basis $\{|00\rangle,|01\rangle,|10\rangle,|11\rangle\}$ the concurrence is simply given by

$$C(t) = 2|\rho_{12}(t)|. \tag{43}$$

It turns out that the decay characteristics of the density matrix element ρ_{12} depend on the initial two-resonator state. In particular, the time evolution of the concurrences $C_{\pm}(t)$ for the initial density operators $(|\psi_{\pm}\rangle\langle\psi_{\pm}|)_{\mathrm{cav}}$ is found as

$$C_+(t) = e^{-(\kappa+2\kappa_{\mathrm{qb}})t}, \tag{44}$$

$$C_-(t) = e^{-\kappa t}. \tag{45}$$

The reason for this particular behavior is that the state $|\psi_-\rangle_{\mathrm{cav}}$ lies in a decoherence-free subspace with respect to the dissipator $D[a+b]$. Thus, it is a robust state in the sense that it does not couple to the qubit-induced correlated noise source.[62,63] This statement is equivalent to the relation $D[a+b](|\psi_-\rangle\langle\psi_-|)_{\mathrm{cav}}=0$. On the contrary, the initial state $|\psi_+\rangle_{\mathrm{cav}}$ is fragile in this respect, since $D[a+b](|\psi_+\rangle\langle\psi_+|)_{\mathrm{cav}}\neq 0$.

In Fig. 7, we compare the numerically calculated time evolution of the concurrence to the analytical results of Eqs. (44) and (45), finding good agreement. While the decay of $C_+(t)$ is enhanced due to the qubit dissipation channel, the time evolution of $C_-(t)$ is determined by resonator dissipation only (cf. Figure 7), in analogy to the findings of Eqs. (38) and (39). We note that a corresponding behavior has been reported for correlated states of a chain of coupled qubits interacting with a common bath.[64] The numerical result

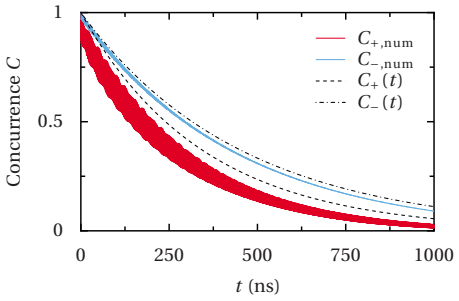

FIG. 7. (Color online) Decay of concurrence C_+ and C_- for the entangled initial states $|\psi_+\rangle_{\mathrm{cav}}$ and $|\psi_-\rangle_{\mathrm{cav}}$ (solid red lines, thick curve, and solid blue lines, thin curve, respectively). The switch-setting off condition $g_{\mathrm{SW}}=0$ is fulfilled by $\varepsilon/2\pi=-8.916$ GHz$/2\pi$. Here we use $G=0.00478$ GHz, all other parameters are as in Fig. 3. The exponential decay corresponds to Eqs. (44) and (45) (black dashed and dash-dotted lines, respectively).

is found to be shifted with respect to the analytical curves, since other elements of the density operator, e.g., ρ_{33} become populated as well during the time evolution of the system state. This non-RWA feature stems from the full numerical treatment using the system Hamiltonian Eq. (1).

These findings can now be employed to characterize the decay of entanglement for the initial states $|\psi_{\pm}^i\rangle_{\mathrm{cav}}$. For this purpose we express them as linear superpositions of the Bell states $|\psi_{\pm}\rangle_{\mathrm{cav}}$ [Eq. (42)],

$$|\psi_{\pm}^i\rangle_{\mathrm{cav}} = \frac{1}{2}[(1+i)|\psi_+\rangle + (1\pm i)|\psi_-\rangle]_{\mathrm{cav}}. \tag{46}$$

Consistently, we find that the analogously defined concurrences $C_{\pm}^i$ can be expressed as a sum of the concurrences of the initial Bell states [Eqs. (44) and (45)] as

$$C_+^i(t) = C_-^i(t) = \frac{1}{2}(e^{-(\kappa+2\kappa_{\mathrm{qb}})t} + e^{-\kappa t}). \tag{47}$$

This has some interesting consequences. For short times, the decay out of both initial states $|\psi_{\pm}^i\rangle_{\mathrm{cav}}$ is merely governed by qubit-enhanced decay at a rate $\kappa+2\kappa_{\mathrm{qb}}$. In the limit of long times, however, one finds pure resonator decay at a rate κ. We have confirmed this numerically in Fig. 8 by means of the concurrence $C_+^i(t)$ related to the initial state $|\psi_+^i\rangle_{\mathrm{cav}}$.

In summary, we point out that it is possible to understand the time evolution characteristics of the entanglement in the system on the basis of the effective master equation (34). We emphasize that the qubit-induced dissipation channel plays a crucial, selective role for different classes of initially entangled states.

V. EXTRACTING DAMPING CONSTANTS BY (CROSS-) CORRELATIONS

In the two-resonator setup, it is possible to measure correlations and cross-correlations in terms of the expectation values $\langle(a+a^\dagger)^2\rangle$, $\langle(b+b^\dagger)^2\rangle$, and $\langle(a+a^\dagger)(b+b^\dagger)\rangle$ with present techniques.[65] In the following we propose a method how to extract the relaxation rates κ and κ_{qb} out of correlation measurements of such type. We define the oscillator

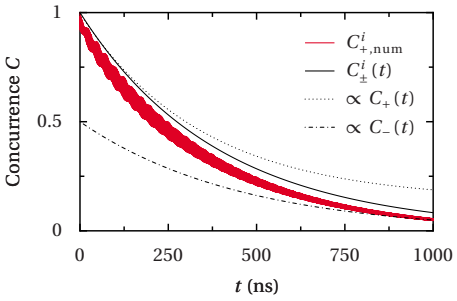

FIG. 8. (Color online) Decay of concurrence C^i_+ for the entangled initial state $|\psi^i_+\rangle_{\mathrm{cav}}$ (red solid lines, thick curve). The switch-setting off condition $g_{\mathrm{SW}}=0$ is fulfilled by $\varepsilon/2\pi=-8.916$ GHz. Here we use $G=0.00478$ GHz, all other parameters as in Fig. 3. The two-mode exponential (solid black line) corresponds to Eq. (47). The additional exponentials are given by Eqs. (44) and (45) and highlight the different decay regimes.

"positions" $X_A=a+a^\dagger$ and $X_B=b+b^\dagger$. In analogy to Sec. IV B, we find analytically that the quantity $\langle X_-^2\rangle=\langle X_A^2\rangle+\langle X_B^2\rangle-2\langle X_AX_B\rangle$ decays at the rate κ. For $\langle X_+^2\rangle=\langle X_A^2\rangle+\langle X_B^2\rangle+2\langle X_AX_B\rangle$ we find a decay with $\kappa+2\kappa_{\mathrm{qb}}$. In Fig. 9, we numerically substantiate these findings for the example of a coherent initial state $|g\rangle_{\mathrm{qb}}|\alpha=1\rangle_A|\beta=0\rangle_B$, discarding again transient effects.

Thus, we point out the possibility to extract the resonator decay rate κ by measuring the decay of $\langle X_-^2\rangle$. This allows in turn for deducing the rate κ_{qb} related to qubit-enhanced decay by measuring the quantity $\langle X_+^2\rangle$. From the latter measurement, it is further possible to gain information about the

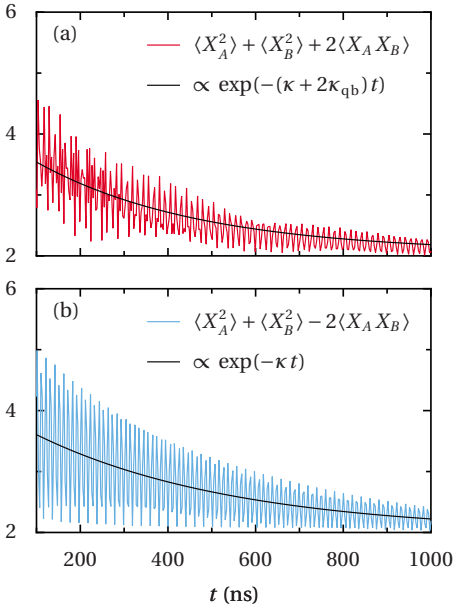

FIG. 9. (Color online) Time evolution of the auto-correlations and cross-correlations of the initial state $|g\rangle_{\mathrm{qb}}|\alpha=1\rangle_A|\beta=0\rangle_B$: Decay of $\langle X_A^2\rangle+\langle X_B^2\rangle+2\langle X_AX_B\rangle$ [panel (a), red solid lines, oscillating] and $\langle X_A^2\rangle+\langle X_B^2\rangle-2\langle X_AX_B\rangle$ [panel (b), blue solid lines, oscillating]. The exponential decay is compared to the analytical estimates given by Eqs. (38) and (39) (black solid lines). Initial transient effects are not depicted in the figure. For parameters and initial conditions, see Fig. 3 and 6, respectively.

relaxation and dephasing rates of the qubit, $\gamma(\omega_{\mathrm{qb}})$ [Eq. (13)] and $\gamma_\phi(\omega\to 0)$, [Eq. (14)], provided that the system frequencies and resonator-qubit interaction strengths are known. More details about a possible experimental realization of such correlation measurements can be found in Refs. 66 and 67.

VI. CONCLUSIONS

We have investigated a two-resonator circuit QED setup in the dispersive regime, i.e., for a resonator-qubit detuning much larger than their mutual coupling. There, it is possible to extract the relevant system dynamics by applying the unitary transformation (23) to the system Hamiltonian (5). The resulting effective Hamiltonian (28) reveals that the qubit gives rise to a switchable coupling between the resonators via virtual excitations. This dynamical coupling adds to the direct resonator-resonator coupling. Balancing both contributions, the resonator-resonator interaction can be set to zero. Such a qubit-mediated interaction provides a physical realization for a quantum switch between the resonators.

As a principal point, we have focused on the dissipative system properties that stem from the interaction with different environments. For weak system-bath coupling, it is possible to cast the time evolution of the reduced system state into a quantum master equation of Bloch-Redfield form, Eq. (9). It is usually derived starting from the total microscopic system-bath Hamiltonian, Eq. (8). Its character being quite general, it only offers limited analytic insight. To study the dissipative dynamics in the dispersive regime, it is preferable to obtain a more useful, effective analytical description of the dissipative system dynamics. To this end, we have applied the unitary transformation Eq. (23) to the total system-bath Hamiltonian (8) and analogously obtained the transformed, effective system-bath coupling operators. Applying standard methods, we have derived a rather complex effective quantum master equation for the system state in the rotated frame. It can be simplified, however, assuming low temperatures and recalling that the qubit state does not change, and only the dynamics of the two-resonator system are of relevance. By tracing out the qubit degrees of freedom one arrives at the Lindblad-type quantum master equation (34) for the reduced two-resonator state.

As a main result, we have found that the qubit induces decoherence on the resonator-resonator system via an additional noise channel that acts on the "center of mass coordinate" of the resonators. This effect stems from qubit energy relaxation and is of second order in the small dispersive parameters $\lambda_{\{\Delta,\Sigma\}}$, whereas pure qubit dephasing only enters in fourth order. This result anticipates that the operation of the quantum switch is robust against low-frequency noise in the two-level system. For reasons of clearness, our findings are again illustrated in Fig. 10. We have verified our analytical findings by numerical calculations, where we have taken into account the full dissipative dynamics according to Eq. (9). As detailed in Sec. IV by means of several examples, we have found an excellent agreement of the presented dispersive theory and the numerical results. Here, in particular, we have investigated the validity of the obtained resonator re-

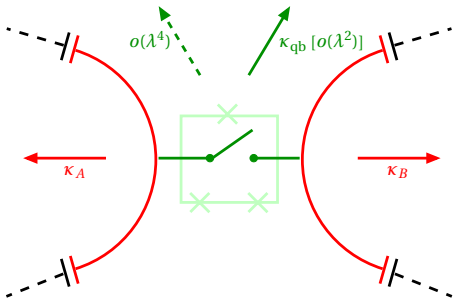

FIG. 10. (Color online) Sketch of the relevant decay mechanisms affecting the quantum switch. The qubit induces extra decoherence in higher dispersive order to the effective resonator-resonator dynamics. The arrows mark the decoherence channels, labeled by the corresponding decay rates $\kappa_{\{A,B,\mathrm{qb}\}}$. Decay processes of fourth order in the parameters $\lambda_{\{\Delta,\Sigma,\Omega\}}$ are not displayed individually.

laxation rates. With regard to generating entangled states, which is a key application of the quantum switch, we have examined the decay mechanisms for different entangled initial resonator-resonator states.

ACKNOWLEDGMENTS

We gratefully acknowledge financial support by the German Excellence Initiative via the "Nanosystems Initiative Munich (NIM)." E.S. acknowledges funding from UPV/EHU under Grant No. GIU07/40, Ministerio de Ciencia e Innovación under Grant No. FIS2009-12773-C02-01, and European Projects EuroSQIP and SOLID. This work has been supported by the German Research Foundation (DFG) through the Collaborative Research Centers SFB 484 and SFB 631.

APPENDIX A: ENERGY RELAXATION AND PURE DEPHASING RATES OF THE QUBIT

In this section, we derive a quantum master equation for the qubit alone, which allows us to identify the energy relaxation and pure dephasing rates of the qubit. Considering only a qubit coupled to individual environments along the σ_x' and σ_z'-axes in the laboratory frame, the qubit-bath Hamiltonian reads

$$\mathcal{H}'_{\mathrm{tot,qb}} = \mathcal{H}'_{\mathrm{qb}} + \sum_{\mu=x,z} Q_\mu \sum_j c_j^\mu (d_{j,\mu}^\dagger + d_{j,\mu}) + \sum_{\mu=x,z}\sum_j \hbar\omega_j^\mu \left(d_{j,\mu}^\dagger d_{j,\mu} + \frac{1}{2} \right), \tag{A1}$$

where $\mathcal{H}'_{\mathrm{qb}} = (\hbar\epsilon/2)\sigma_z' + (\hbar\delta_Q/2)\sigma_x'$. Applying Eq. (4), we obtain the diagonal qubit Hamiltonian $\mathcal{H}_{\mathrm{qb}} = (\hbar\omega_{\mathrm{qb}}/2)\sigma_z$ and also the qubit-bath Hamiltonian,

$$\mathcal{H}_{\mathrm{tot,qb}} = \mathcal{H}_{\mathrm{qb}} + \sum_{\mu=x,z}\sum_j \hbar\omega_j^\mu \left(d_{j,\mu}^\dagger d_{j,\mu} + \frac{1}{2} \right) + (\sin\theta\sigma_z + \cos\theta\sigma_x)\sum_j c_j^x (d_{j,x}^\dagger + d_{j,x}) + (\cos\theta\sigma_z - \sin\theta\sigma_x)\sum_j c_j^z (d_{j,z}^\dagger + d_{j,z}). \tag{A2}$$

Starting from the density matrix $\varrho_{\mathrm{tot,qb}}$ associated with $\mathcal{H}_{\mathrm{tot,qb}}$ and following the lines of Ref. 55, the Lindblad quantum master equation for the reduced qubit density operator $\varrho_{\mathrm{qb}} = \mathrm{Tr}_{\mathrm{bath}}[\varrho_{\mathrm{tot,qb}}]$ can be derived. To this end, the spectral decompositions $\sigma_-(\omega) = \delta(\omega_{\mathrm{qb}} - \omega)\sigma_-$, $\sigma_+(\omega) = \delta(\omega_{\mathrm{qb}} + \omega)\sigma_+$, and $\sigma_z(\omega) = \delta(\omega)\sigma_z$ of the qubit-bath coupling operators are required. Omitting the explicit time dependence of ϱ_{qb} for simplicity, we find

$$\dot{\varrho}_{\mathrm{qb}} = -\frac{i}{\hbar}[\mathcal{H}_{\mathrm{qb}}, \varrho_{\mathrm{qb}}] + \gamma(\omega_{\mathrm{qb}}) \left[\sigma^- \varrho_{\mathrm{qb}} \sigma^+ - \frac{1}{2}[\sigma^+\sigma^-, \varrho_{\mathrm{qb}}]_+ \right] + \gamma(-|\omega_{\mathrm{qb}}|) \left[\sigma^+ \varrho_{\mathrm{qb}} \sigma^- - \frac{1}{2}[\sigma^-\sigma^+, \varrho_{\mathrm{qb}}]_+ \right] + \gamma_\phi(\omega \to 0)[\sigma_z \varrho_{\mathrm{qb}} \sigma_z - \varrho_{\mathrm{qb}}]. \tag{A3}$$

Here, $\sigma_- = |g\rangle\langle e|$ and $\sigma_+ = |e\rangle\langle g|$ are the fermionic qubit annihilation and creation operators. The energy level transition and the pure dephasing rates are given by

$$\gamma(\omega) = \Gamma_x(\omega)\cos^2\theta + \Gamma_z(\omega)\sin^2\theta, \tag{A4}$$

$$\gamma_\phi(\omega) = \Gamma_x(\omega)\sin^2\theta + \Gamma_z(\omega)\cos^2\theta, \tag{A5}$$

respectively, and depend on the bath correlation functions

$$\Gamma_\mu(\omega) = \begin{cases} J_\mu(\omega)(n_\mu(\omega)+1), & \omega \geq 0 \\ J_\mu(|\omega|)n_\mu(|\omega|), & \omega < 0, \end{cases} \tag{A6}$$

where $n_\mu(\omega) = 1/(e^{\hbar\omega/k_{\mathrm{B}}T_\mu} - 1)$ is the Bose distribution function of bath with label $\mu \in \{x,z\}$. Because the quantum switch operates in the limit of low temperatures, $k_{\mathrm{B}}T_\mu \ll \hbar\omega_{\mathrm{qb}}$, the Bose-factor $n_\mu(\omega)$ vanishes for frequencies of the order of ω_{qb}. However, for $\omega \to 0$, $n_\mu(\omega)$ tends to diverge. This can be relevant in the experimentally important case of $1/f$ noise,[31–33] which would require a treatment beyond the framework of a Markovian master equation, exceeding the scope of this work. Instead, we avoid the divergence problem by choosing Ohmic spectral densities [Eq. (11)] for low frequencies $\omega \ll \omega_{\mathrm{qb}}$. In many cases, this assumption is reasonable.[68–70] Provided that both baths have the same temperature $T = T_{\{x,z\}}$, we obtain

$$\gamma(\omega \geq 0) = J_x(\omega)\cos^2\theta + J_z(\omega)\sin^2\theta, \tag{A7}$$

$$\gamma(\omega < 0) \approx 0, \tag{A8}$$

$$\gamma_\phi(\omega \to 0) = \frac{k_{\mathrm{B}}T}{\hbar}(\alpha_z \cos^2\theta + \alpha_x \sin^2\theta). \tag{A9}$$

These rates are functions of the mixing angle θ. Equation (A7) constitutes the main result of this section. For $\omega = \omega_{\mathrm{qb}}$, it establishes the connection between the energy relaxation rate

in the energy eigenframe and the dissipative baths defined in the laboratory frame. The Markovian description of Eq. (A3) remains justified as long as the spectral densities $J_{\{x,z\}}(\omega)$ are smooth functions in ω_{qb}. This allows one to apply a linear approximation in an infinitely small interval around ω_{qb}, which yields an effectively Ohmic description. We finally note that in the special case of noise coupling purely via the laboratory z axis (e.g., a flux qubit exposed to flux noise) the result $\gamma(\omega_{\mathrm{qb}})=J_z(\omega_{\mathrm{qb}})\sin^2\theta$ is in agreement with findings from other works.[32,48,49] For the sake of completeness we mention that the master equation (A3) together with the rates (A7)–(A9) reproduce the well-known results concerning relaxation and pure dephasing times, $(T_1)^{-1}=\gamma(\omega\geq 0)$ and $T_\phi^{-1}=\gamma_\phi(\omega\to 0)$, respectively.

APPENDIX B: EFFECTIVE BATH COUPLING OPERATORS

To obtain the quantum master equation for the reduced system state, it is necessary to transform the total system-bath Hamiltonian to the dispersive picture via the transformation $\mathcal{H}_{\mathrm{tot,eff}}=\mathcal{U}^\dagger\mathcal{H}_{\mathrm{tot}}\mathcal{U}$, with $\mathcal{U}$ given in Eq. (23). The effective system Hamiltonian having been derived in Sec. III B, we need yet to find the transforms (23) of the system-bath coupling operators Q_μ to the dispersive frame. Up to second order in $\lambda_{\{\Delta,\Sigma,\Omega\}}$, they read as

$$\begin{aligned}Q_{\mu,\mathrm{eff}}=\mathcal{U}^\dagger Q_\mu\mathcal{U}=Q_\mu+[Q_\mu,\lambda_\Delta\mathcal{D}+\lambda_\Sigma\mathcal{S}+\lambda_\Omega\mathcal{W}]\\+[[Q_\mu,\lambda_\Delta\mathcal{D}+\lambda_\Sigma\mathcal{S}+\lambda_\Omega\mathcal{W}],\lambda_\Delta\mathcal{D}+\lambda_\Sigma\mathcal{S}+\lambda_\Omega\mathcal{W}]\\+\mathcal{O}(\lambda^3_{\{\Delta,\Sigma,\Omega\}})\quad \mu\in\{A,B,x,z\}.\end{aligned}\tag{B1}$$

Each of the effective bath coupling operators $Q_{\mu,\mathrm{eff}}$ is represented by of a sum of operators,

$$Q_{\mu,\mathrm{eff}}=\sum_{j_\mu}Q_{j_\mu}.$$

For the resonator-bath coupling operators $Q_A=a+a^\dagger$ and $Q_B=b+b^\dagger$, we obtain the dispersive transforms as

$$\begin{aligned}Q_{A,\mathrm{eff}}=(a+a^\dagger)_{\mathrm{eff}}=a+a^\dagger+(\lambda_\Delta-\lambda_\Sigma)\sigma_x-2\lambda_\Omega\sigma_z\\+\frac{1}{2}(\lambda_\Delta^2-\lambda_\Sigma^2)(a+b+a^\dagger+b^\dagger)\\+\lambda_\Omega(\lambda_\Delta+\lambda_\Sigma)\sigma_x(a+b+a^\dagger+b^\dagger),\end{aligned}\tag{B2}$$

$$\begin{aligned}Q_{B,\mathrm{eff}}=(b+b^\dagger)_{\mathrm{eff}}=b+b^\dagger+(\lambda_\Delta-\lambda_\Sigma)\sigma_x-2\lambda_\Omega\sigma_z\\+\frac{1}{2}(\lambda_\Delta^2-\lambda_\Sigma^2)(a+b+a^\dagger+b^\dagger)\\+\lambda_\Omega(\lambda_\Delta+\lambda_\Sigma)\sigma_x(a+b+a^\dagger+b^\dagger).\end{aligned}\tag{B3}$$

The dispersive transforms of the qubit-bath coupling operators $Q_{x,\mathrm{eff}}=\sigma_{x,\mathrm{eff}}$ and $Q_{z,\mathrm{eff}}=\sigma_{z,\mathrm{eff}}$ are obtained as a combination of those of the qubit operators σ_x' and σ_z' in the laboratory basis, according to Eq. (4). The latter assume the form

$$\begin{aligned}\sigma'_{x,\mathrm{eff}}=\sigma_x+(\lambda_\Delta+\lambda_\Sigma)\sigma_z(a+b+a^\dagger+b^\dagger)-2\lambda_\Omega[\sigma^+(a+b)\\+\sigma^-(a^\dagger+b^\dagger)-\sigma^+(a^\dagger+b^\dagger)-\sigma^-(a+b)]\\-((\lambda_\Delta+\lambda_\Sigma)^2-4\lambda_\Omega^2)\sigma_x[(a^\dagger+b^\dagger)(a+b)+1]\\+(2\lambda_\Omega^2-(\lambda_\Delta+\lambda_\Sigma)\lambda_\Delta)[\sigma^-(a^\dagger+b^\dagger)^2+\sigma^+(a+b)^2]\\+\lambda_\Omega(\lambda_\Delta-\lambda_\Sigma)\sigma_z(a+b+a^\dagger+b^\dagger)+(2\lambda_\Omega^2\\-(\lambda_\Delta+\lambda_\Sigma)\lambda_\Sigma)[\sigma^-(a+b)^2+\sigma^+(a^\dagger+b^\dagger)^2],\end{aligned}\tag{B4}$$

$$\begin{aligned}\sigma'_{z,\mathrm{eff}}=\sigma_z-2\lambda_\Delta[\sigma^+(a+b)+\sigma^-(a^\dagger+b^\dagger)]-2\lambda_\Sigma[\sigma^+(a^\dagger+b^\dagger)\\+\sigma^-(a+b)]-2\sigma_z(\lambda_\Delta^2+\lambda_\Sigma^2)[(a^\dagger+b^\dagger)(a+b)+1]\\+4\lambda_\Omega(\lambda_\Delta-\lambda_\Sigma)\sigma_x[(a^\dagger+b^\dagger)(a+b)+1]\\+4\lambda_\Omega\lambda_\Delta[\sigma^+(a+b)^2+\sigma^-(a^\dagger+b^\dagger)^2]+4\lambda_\Omega\lambda_\Sigma[\sigma^-(a\\+b)^2+\sigma^+(a^\dagger+b^\dagger)^2]-2\lambda_\Delta\lambda_\Sigma\sigma_z[(a+b)^2+(a^\dagger+b^\dagger)^2].\end{aligned}\tag{B5}$$

APPENDIX C: EFFECTIVE QUANTUM MASTER EQUATION IN THE DISPERSIVE LIMIT

Starting from the Bloch-Redfield quantum master equation (9), we move to an interaction picture with respect to the system and the individual reservoirs. Here, the coupling operators Q_μ have to be replaced by their dispersive transforms $Q_{\mu,\mathrm{eff}}$ found in Appendix B. Now, we introduce the spectral decompositions

$$Q_{\mu,\mathrm{eff}}\equiv\sum_{j_\mu}Q_{j_\mu}=\sum_{j_\mu}\sum_{\omega}Q_{j_\mu}(\omega).\tag{C1}$$

The Q_{j_μ} are the summands of the effective coupling operators as detailed in Eqs. (B2)–(B5). The spectral components $Q_{j_\mu}(\omega)$ are obtained by expanding the Q_{j_μ} in terms of the eigenstates of the effective Hamiltonian (28), which we cast in entirely diagonal form for this reason,

$$\mathcal{H}_{\mathrm{eff}}=\hbar\hat{\tilde{\Omega}}_+\left(A_+^\dagger A_+-\frac{1}{2}\right)+\hbar\tilde{\Omega}_-\left(A_-^\dagger A_--\frac{1}{2}\right)+\frac{\hbar\tilde{\epsilon}}{2},\tag{C2}$$

Here we have defined

$$\hat{\tilde{\Omega}}_+=\Omega+G+2(\lambda_\Delta\Delta+\lambda_\Sigma\Sigma)\sigma_z,\tag{C3}$$

$$\tilde{\Omega}_-=\Omega-G,\tag{C4}$$

$$\tilde{\epsilon}=\omega_{\mathrm{qb}}+2(\lambda_\Delta\Delta+\lambda_\Sigma\Sigma),\tag{C5}$$

and introduced via a linear transformation the normal modes

$$A_+=\frac{1}{\sqrt{2}}(a+b),\quad A_-=\frac{1}{\sqrt{2}}(a-b).\tag{C6}$$

The eigenstates of the effective Hamiltonian (C2) can be considered as re-defined Fock states,

$$\mathcal{H}_{\rm eff}|nml\rangle = \frac{\hbar\tilde{\epsilon}}{2}(-1)^{l+1}|l\rangle + \hbar\tilde{\Omega}_+(l)\left(n+\frac{1}{2}\right)|n\rangle + \hbar\tilde{\Omega}_-\left(m+\frac{1}{2}\right)|m\rangle. \tag{C7}$$

Here, $\{n,m\}=\{0,1,2,\ldots\}$ denote the oscillator excitations (or resonator photon numbers), and $\tilde{\Omega}_A(l)$ can assume the values

$$\tilde{\Omega}_+(l) = \Omega + G + 2(\lambda_\Delta\Delta + \lambda_\Sigma\Sigma)(-1)^{l+1} \tag{C8}$$

with $l=1$ or $l=0$ for the qubit being in the excited or ground state, respectively. With this at hand we find the spectral decompositions of the effective coupling operators via the ansatz

$$Q_{j_\mu}(\omega) = \sum_{nml}\sum_{n'm'l'}\delta(\Delta_{nml}^{n'm'l'} - \omega) \times |nml\rangle\langle nml|Q_{j_\mu}|n'm'l'\rangle\langle n'm'l'|, \tag{C9}$$

where $\Delta_{nml}^{n'm'l'}$ denotes the energy difference between the states $|n'm'l'\rangle$ and $|nml\rangle$. For illustration we list the explicit expressions for the spectral decompositions of some components,

$$A_+(\omega) = A_+|0\rangle\langle 0|\,\delta(\omega - \tilde{\Omega}_+(0)) + A|1\rangle\langle 1|\,\delta(\omega - \tilde{\Omega}_+(1)), \tag{C10}$$

$$A_-(\omega) = A_-\delta(\omega - \tilde{\Omega}_-), \tag{C11}$$

$$\sigma^-(\omega) = \sigma^-\sum_n |n\rangle\langle n|\,\delta(\omega - [\omega_{\rm qb} + (2n+1)(\lambda_\Delta^2\Delta + \lambda_\Sigma^2\Sigma)]), \tag{C12}$$

$$\sigma_z(\omega) = \sigma_z\delta(\omega). \tag{C13}$$

The decompositions of operator products such as $\sigma^-A_+^\dagger$ etc. are obtained analogously via the relation $Q_{j_\mu}^\dagger(\omega) = Q_{j_\mu}(-|\omega|)$. With this and Eq. (C1), we recast the Bloch-Redfield quantum master equation (9) into the form

$$\dot{\rho}(t) = -\frac{i}{\hbar}[\mathcal{H}_{\rm eff},\rho(t)] + \sum_\mu\sum_{j_\mu,k_\mu}\sum_{\omega,\omega'} e^{i(\omega'-\omega)t}\Gamma_\mu(\omega) \times (Q_{j_\mu}(\omega)\varrho(t)Q_{k_\mu}^\dagger(\omega') - Q_{k_\mu}^\dagger(\omega')Q_{j_\mu}(\omega)\varrho(t)) + \text{H.c.}, \tag{C14}$$

where $\Gamma_\mu(\omega)$ is the one-sided Fourier transform

$$\Gamma_\mu(\omega) \equiv \int_0^\infty d\tau e^{i\omega\tau}K_\mu(\tau) \tag{C15}$$

of the bath correlation function $K_\mu(\tau)$ given in Eq. (10). One usually neglects the Cauchy principal value of the integral and can then rewrite Eq. (C15) as

$$\Gamma_\mu(\omega) = \begin{cases} J_\mu(\omega)(n_\mu(\omega)+1), & \omega \geq 0 \\ J_\mu(|\omega|)n_\mu(\omega), & \omega < 0, \end{cases} \tag{C16}$$

with the spectral density $J_\mu(\omega)$ and the Bose distribution function $n_\mu(\omega)=1/(e^{\hbar\omega/k_{\rm B}T_\mu}-1)$, depending on the temperatures T_μ.

Inserting the explicit expressions for the spectral decompositions into the quantum master equation (C14), we find two different classes of oscillating terms. The first oscillate at high frequencies such as $e^{\pm i\tilde{\Omega}_{A/B}t}, e^{\pm i\omega_{\rm qb}t}, e^{\pm i\Delta t}, e^{\pm i\Sigma t}$, i.e., vary on time scales of the intrinsic system evolution, whereas the second oscillate slowly at frequencies $\lambda_\Delta^2\Delta + \lambda_\Sigma^2\Sigma$ and multiples. This difference enables one to perform a semisecular approximation similar to the approach in Ref. 56. Here, we assume that all rapidly oscillating terms of the first class can be averaged to zero. This is justified since the time scales of intrinsic system evolution given by $(\tilde{\Omega}_{\{A,B\}})^{-1}$ etc. are typically much smaller than the relaxation time scales, on which the system state varies notably. This, however, is not the case for terms of the second class, which we keep consistently. We emphasize that our approach goes beyond the standard way of obtaining a Lindblad quantum master equation. The latter would imply a full secular approximation, neglecting *all* oscillating contributions and only keeping terms with $\omega=\omega'$ in Eq. (C14).

Furthermore, we may simplify the bath correlation functions,

$$\Gamma(\tilde{\Omega}_A(0)) \approx \Gamma(\tilde{\Omega}_A(1)) \approx \Gamma(\tilde{\Omega}_B) \approx \Omega,$$

$$\Gamma(\omega_{\rm qb} + n(\lambda_\Delta^2\Delta + \lambda_\Sigma^2\Sigma)) \approx \Gamma(\omega_{\rm qb})$$

for small occupation numbers n, and assume an overall temperature $T=T_{\{A,B,x,z\}}$. In the low-temperature regime, $T \ll (\hbar/k_{\rm B})\min\{\omega_{\rm qb},\Delta,\Omega\}$, it is appropriate to neglect all contributions to Eq. (C14) with negative frequencies because of $\Gamma_\mu(\omega<0)\approx 0$, i.e., no energy is absorbed from the baths. This automatically yields $\Gamma_\mu(\omega)=J_\mu(\omega)$. In the low-frequency region of the qubit baths, we assume Ohmic spectral behavior, $J_{\{x,z\}}(\omega)=\alpha_{\{x,z\}}\omega$. As detailed in Appendix A, this implies $\Gamma_{\{x,z\}}(\omega\to 0)=\alpha_{\{x,z\}}k_{\rm B}T/\hbar$.

We eventually obtain the effective quantum master equation for the reduced system state

$$\begin{aligned}\dot{\rho} = &-\frac{i}{\hbar}[\mathcal{H}_{\rm eff},\rho] + J_A(\Omega)D[a]\rho + J_B(\Omega)D[b]\rho \\ &+ (\lambda_\Delta+\lambda_\Sigma)^2(J_x(\Omega)\cos^2\theta + J_z(\Omega)\sin^2\theta)D[\sigma_z(a+b)]\rho \\ &+ J_x(\omega_{\rm qb})D[\sigma^-(\cos\theta - (\cos\theta(-4\lambda_\Omega^2 + (\lambda_\Delta+\lambda_\Sigma)^2) \\ &+ 4\sin\theta\lambda_\Omega(\lambda_\Delta-\lambda_\Sigma))((a^\dagger+b^\dagger)(a+b)+1))]\rho \\ &+ J_x(\omega_{\rm qb})D[\sigma^-(-\sin\theta + (\sin\theta(-4\lambda_\Omega^2 + (\lambda_\Delta+\lambda_\Sigma)^2) \\ &- 4\cos\theta\lambda_\Omega(\lambda_\Delta-\lambda_\Sigma))((a^\dagger+b^\dagger)(a+b)+1))]\rho \\ &+ 4(J_x(\Delta)(\lambda_\Omega\cos\theta + \lambda_\Delta\sin\theta)^2 + J_z(\Delta)(\lambda_\Delta\cos\theta \\ &- \lambda_\Omega\sin\theta)^2)D[\sigma^-(a^\dagger+b^\dagger)]\rho + 4(J_x(\Sigma)(\lambda_\Omega\cos\theta \\ &- \lambda_\Sigma\sin\theta)^2 + J_z(\Sigma)(\lambda_\Sigma\cos\theta + \lambda_\Omega\sin\theta)^2)D[\sigma^-(a+b)]\rho\end{aligned}$$

$$+(k_BT/\hbar)(\alpha_x \sin^2\theta+\alpha_z\cos^2\theta)D[\sigma_z(1-2(\lambda_\Delta^2+\lambda_\Sigma^2)\times((a^\dagger+b^\dagger)(a+b)+1))]\rho, \quad \text{(C17)}$$

where we have omitted the time dependence of the density operator ρ and used the notation $D[X]\rho=X\varrho X^\dagger-\frac{1}{2}[X^\dagger X,\varrho]_+$ with the anticommutator $[\mathcal{A},\mathcal{B}]_+=\mathcal{A}\mathcal{B}+\mathcal{B}\mathcal{A}$.

We have neglected terms $\propto\lambda^2_{\{\Delta,\Sigma,\Omega\}}J_{\{A,B\}}(\omega)$ and higher orders of $\lambda_{\{\Delta,\Sigma,\Omega\}}$ in Eq. (C17). This is justified, since the resonators typically employed in experiment possess a high quality factor and therefore feature small decay rates. On the other hand, it is necessary to keep terms proportional to $\lambda^2_{\{\Delta,\Sigma,\Omega\}}J_{\{x,z\}}(\omega)$, because typical qubit dephasing and relaxation rates exceed those of the resonators by several orders of magnitude with conservative estimates. In general, it is appropriate to neglect all terms of the order of $\lambda^3_{\{\Delta,\Sigma,\Omega\}}$ and higher. Due to the dissipator relation $D[\lambda X]=\lambda^2 D[X]$ we thus may already discard any contributions to the system-bath coupling operators of order $\lambda^2_{\{\Delta,\Sigma,\Omega\}}$ in Eqs. (B2)–(B5).

In Sec. III A we have motivated the experimental advantage of keeping the qubit in its ground state without own dynamics. This enables us to simplify Eq. (C17) further by tracing out the qubit degrees of freedom. To this end, we take into account $\mathrm{Tr}(\sigma_z|g\rangle\langle g|)=-1$ and the partial trace relation

$$\mathrm{Tr}_1(D[A_1\otimes A_2]\rho)=\mathrm{Tr}_1(A_1^\dagger A_1 D[A_2]\rho), \quad \text{(C18)}$$

with A_1 and A_2 acting each on a different Hilbert subspace, and $\mathrm{Tr}_1(\cdot)$ denoting the partial trace with respect to one subspace. Finally, we arrive at the effective quantum master equation for the tow-resonator state, Eq. (34). The qubit decoherence rates γ_x and γ_ϕ are identified following the discussion in Appendix A.

*georg.reuther@physik.uni-augsburg.de
†david.zueco@physik.uni-augsburg.de
‡Present address: Department of Physics, University of California, Santa Barbara, California 93106, USA.

[1] A. Wallraff, D. I. Schuster, A. Blais, L. Frunzio, R.-S. Huang, J. Majer, S. Kumar, S. M. Girvin, and R. J. Schoelkopf, Nature (London) **431**, 162 (2004).
[2] A. Blais, R.-S. Huang, A. Wallraff, S. M. Girvin, and R. J. Schoelkopf, Phys. Rev. A **69**, 062320 (2004).
[3] J. Q. You and F. Nori, Phys. Today **58** (11), 42 (2005).
[4] R. J. Thompson, G. Rempe, and H. J. Kimble, Phys. Rev. Lett. **68**, 1132 (1992).
[5] H. Mabuchi and A. C. Doherty, Science **298**, 1372 (2002).
[6] S. Haroche and J.-M. Raimond, *Exploring the Quantum* (Oxford University Press Inc., New York, 2006).
[7] Y. Makhlin and A. D. Mirlin, Phys. Rev. Lett. **87**, 276803 (2001).
[8] G. Wendin and V. S. Shumeiko, in *Handbook of Theoretical and Computational Nanotechnology*, edited by M. Rieth and W. Schommers (American Scientific Publishers, Los Angeles, 2006), Vol. 3, p. 223.
[9] J. Clarke and F. K. Wilhelm, Nature (London) **453**, 1031 (2008).
[10] M. Göppl, A. Fragner, M. Baur, R. Bianchetti, S. Filipp, J. M. Fink, P. J. Leek, G. Puebla, L. Steffen, and A. Wallraff, J. Appl. Phys. **104**, 113904 (2008).
[11] T. Niemczyk, F. Deppe, M. Mariantoni, E. P. Menzel, E. Hoffmann, G. Wild, L. Eggenstein, A. Marx, and R. Gross, Supercond. Sci. Technol. **22**, 034009 (2009).
[12] T. Lindström, C. H. Webster, J. E. Healey, M. S. Colclough, C. M. Muirhead, and A. Y. Tzalenchuk, Supercond. Sci. Technol. **20**, 814 (2007).
[13] J. Q. You and F. Nori, Phys. Rev. B **68**, 064509 (2003).
[14] Y.-X. Liu, L. F. Wei, J. S. Tsai, and F. Nori, Phys. Rev. Lett. **96**, 067003 (2006).
[15] O. Astafiev, K. Inomata, A. O. Niskanen, T. Yamamoto, Yu. A. Pashkin, Y. Nakamura, and J. S. Tsai, Nature (London) **449**, 588 (2007).
[16] A. A. Houck, *et al.*, Nature (London) **449**, 328 (2007).
[17] P. J. Leek, J. M. Fink, A. Blais, R. Bianchetti, M. Göppl, J. M. Gambetta, D. I. Schuster, L. Frunzio, R. J. Schoelkopf, and A. Wallraff, Science **318**, 1889 (2007).
[18] D. I. Schuster, *et al.*, Nature (London) **445**, 515 (2007).
[19] L. S. Bishop, J. M. Chow, J. Koch, A. A. Houck, M. H. Devoret, E. Thuneberg, S. M. Girvin, and R. J. Schoelkopf, Nat. Phys. **5**, 105 (2009).
[20] F. Deppe, *et al.*, Nat. Phys. **4**, 686 (2008).
[21] J. M. Fink, M. Göppl, M. Baur, R. Bianchetti, P. J. Leek, A. Blais, and A. Wallraff, Nature (London) **454**, 315 (2008).
[22] M. Hofheinz, *et al.*, Nature (London) **459**, 546 (2009).
[23] J. Majer, *et al.*, Nature (London) **449**, 443 (2007).
[24] M. A. Sillanpää, J. I. Park, and R. W. Simmonds, Nature (London) **449**, 438 (2007).
[25] L. DiCarlo *et al.*, Nature (London) **460**, 240 (2009).
[26] J. M. Fink, R. Bianchetti, M. Baur, M. Göppl, L. Steffen, S. Filipp, P. J. Leek, A. Blais, and A. Wallraff, Phys. Rev. Lett. **103**, 083601 (2009).
[27] M. Mariantoni, F. Deppe, A. Marx, R. Gross, F. K. Wilhelm, and E. Solano, Phys. Rev. B **78**, 104508 (2008).
[28] P. Xue, B. C. Sanders, A. Blais, and K. Lalumière, Phys. Rev. A **78**, 042334 (2008).
[29] F. Helmer, M. Mariantoni, A. G. Fowler, J. von Delft, E. Solano, and F. Marquardt, EPL **85**, 50007 (2009).
[30] P. Bertet, I. Chiorescu, G. Burkard, K. Semba, C. J. P. M. Harmans, D. P. DiVincenzo, and J. E. Mooij, Phys. Rev. Lett. **95**, 257002 (2005).
[31] F. Yoshihara, K. Harrabi, A. O. Niskanen, Y. Nakamura, and J. S. Tsai, Phys. Rev. Lett. **97**, 167001 (2006).
[32] F. Deppe, M. Mariantoni, E. P. Menzel, S. Saito, K. Kakuyanagi, H. Tanaka, T. Meno, K. Semba, H. Takayanagi, and R. Gross, Phys. Rev. B **76**, 214503 (2007).
[33] K. Kakuyanagi, T. Meno, S. Saito, H. Nakano, K. Semba, H. Takayanagi, F. Deppe, and A. Shnirman, Phys. Rev. Lett. **98**, 047004 (2007).
[34] A. A. Houck, *et al.*, Phys. Rev. Lett. **101**, 080502 (2008).
[35] J. E. Mooij, T. P. Orlando, L. Levitov, L. Tian, C. H. van der Wal, and S. Lloyd, Science **285**, 1036 (1999).
[36] T. P. Orlando, J. E. Mooij, L. Tian, C. H. van der Wal, L. S. Levitov, S. Lloyd, and J. J. Mazo, Phys. Rev. B **60**, 15398

(1999).
[37] B. Yurke and J. S. Denker, Phys. Rev. A **29**, 1419 (1984).
[38] G.-L. Ingold and Yu. V. Nazarov, *Charge Tunneling Rates in Ultrasmall Junctions*, NATO ASI Series B, (Plenum, New York, 1992), Vol. 294, pp. 21–107.
[39] A. O. Caldeira and A. L. Leggett, Ann. Phys. (N.Y.) **149**, 374 (1983).
[40] P. Hänggi, P. Talkner, and M. Borkovec, Rev. Mod. Phys. **62**, 251 (1990).
[41] U. Weiss, *Quantum Dissipative Systems*, Series in Modern Condensed Matter Physics (World Scientific, Singapore, 1993), Vol. 2.
[42] C. Cohen-Tannoudji, J. Dupont-Roc, and G. Grynberg, *Atom-Photon Interaction: Basic Processes and Applications* (Wiley, New York, 1992).
[43] J. Gao, J. Zmuidzinas, B. A. Mazin, H. G. LeDuc, and P. K. Day, Appl. Phys. Lett. **90**, 102507 (2007).
[44] J. Gao, M. Daal, J. M. Martinis, A. Vayonakis, J. Zmuidzinas, B. Sadoulet, B. A. Mazin, P. K. Day, and H. G. LeDuc, Appl. Phys. Lett. **92**, 212504 (2008).
[45] H. Wang, M. Hofheinz, M. Ansmann, R. C. Bialczak, E. Lucero, M. Neeley, A. D. O'Connell, D. Sank, J. Wenner, A. N. Cleland, and J. M. Martinis, Phys. Rev. Lett. **101**, 240401 (2008).
[46] A. G. Redfield, IBM J. Res. Dev. **1**, 19 (1957).
[47] K. Blum, *Density Matrix Theory and Applications*, 2nd ed. (Springer, New York, 1996).
[48] G. Ithier, E. Collin, P. Joyez, D. Vion, D. Esteve, J. Ankerhold, and H. Grabert, Phys. Rev. Lett. **94**, 057004 (2005).
[49] J. Schriefl, Y. Makhlin, A. Shnirman, and G. Schön, New J. Phys. **8**, 1 (2006).
[50] E. T. Jaynes and F. W. Cummings, Proc. IEEE **51**, 89 (1963).
[51] S. Schneider, A. M. Herkommer, U. Leonhardt, and W. P. Schleich, J. Mod. Opt. **44**, 2333 (1997).
[52] D. Zueco, G. M. Reuther, S. Kohler, and P. Hänggi, Phys. Rev. A **80**, 033846 (2009).
[53] M. Boissonneault, J. M. Gambetta, and A. Blais, Phys. Rev. A **77**, 060305(R) (2008).
[54] M. Boissonneault, J. M. Gambetta, and A. Blais, Phys. Rev. A **79**, 013819 (2009).
[55] H. P. Breuer, B. Kappler, and F. Petruccione, *The Theory of Open Quantum Systems* (Oxford University Press, Oxford, 2002).
[56] M. Scala, B. Militello, A. Messina, S. Maniscalco, J. Piilo, and K. A. Suominen, J. Phys. A **40**, 14527 (2007).
[57] M. Hofheinz, E. M. Weig, M. Ansmann, R. C. Bialczak, E. Lucero, M. Neeley, A. D. O'Connell, H. Wang, J. M. Martinis, and A. N. Cleland, Nature (London) **454**, 310 (2008).
[58] J. Johansson, S. Saito, T. Meno, H. Nakano, M. Ueda, K. Semba, and H. Takayanagi, Phys. Rev. Lett. **96**, 127006 (2006).
[59] Y.-X. Liu, L. F. Wei, and F. Nori, Europhys. Lett. **67**, 941 (2004).
[60] D. Zueco, P. Hänggi, and S. Kohler, New J. Phys. **10**, 115012 (2008).
[61] W. K. Wootters, Phys. Rev. Lett. **80**, 2245 (1998).
[62] R. Doll, M. Wubs, P. Hänggi, and S. Kohler, Europhys. Lett. **76**, 547 (2006).
[63] R. Doll, M. Wubs, P. Hänggi, and S. Kohler, Phys. Rev. B **76**, 045317 (2007).
[64] T. Ojanen, A. O. Niskanen, Y. Nakamura, and A. A. Abdumalikov, Phys. Rev. B **76**, 100505(R) (2007).
[65] M. Mariantoni, M. J. Storcz, F. K. Wilhelm, W. D. Oliver, A. Emmert, A. Marx, R. Gross, H. Christ, and E. Solano, arXiv:cond-mat/0509737 (unpublished).
[66] E. P. Menzel, F. Deppe, M. Mariantoni, M. A. Araque Caballero, A. Baust, T. Niemczyk, E. Hoffmann, A. Marx, E. Solano, and R. Gross, arXiv:1001.3669 (unpublished).
[67] M. Mariantoni, E. P. Menzel, F. Deppe, M. A. Araque Caballero, A. Baust, T. Niemczyk, E. Hoffmann, E. Solano, A. Marx, and R. Gross, arXiv:1003.3194 (unpublished).
[68] C. H. van der Wal, Ph.D. thesis, TU Delft, 2001.
[69] C. H. van der Wal, F. K. Wilhelm, C. J. P. M. Harmans, and J. E. Mooij, Eur. Phys. J. B **31**, 111 (2003).
[70] M. Thorwart, E. Paladino, and M. Grifoni, Chem. Phys. **296**, 333 (2004).